Electronic Textiles

International Edition: DOI: 10.1002/anie.201507333
German Edition: DOI: 10.1002/ange.201507333

Smart Electronic Textiles

Wei Weng[+], Peining Chen[+], Sisi He, Xuemei Sun, and Huisheng Peng**

Keywords:
electricity · energy conversation · energy storage · sensors · smart textiles

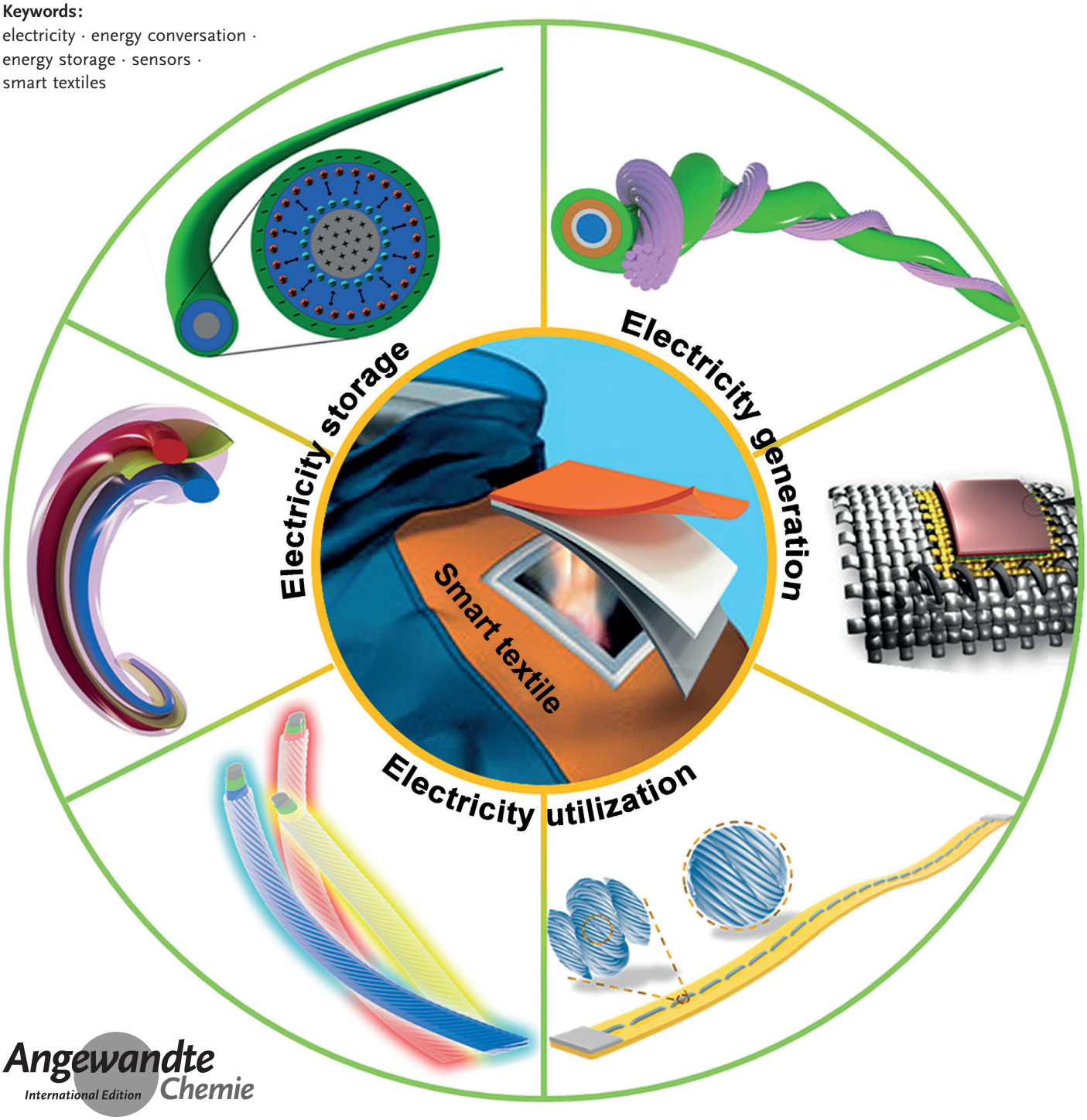

This Review describes the state-of-the-art of wearable electronics (smart textiles). The unique and promising advantages of smart electronic textiles are highlighted by comparing them with the conventional planar counterparts. The main kinds of smart electronic textiles based on different functionalities, namely the generation, storage, and utilization of electricity, are then discussed with an emphasis on the use of functional materials. The remaining challenges are summarized together with important new directions to provide some useful clues for the future development of smart electronic textiles.

From the Contents

1. Introduction

The development of textiles reflects the civilization of humans to a certain extent: A variety of leaves were connected by our ancestors to form the early models of textiles; natural materials such as silk and cotton were then woven into real textiles that were warmer and more comfortable; a broad spectrum of man-made fiber materials, for example, nylon and Kevlar, gradually appeared and greatly enhanced our lives over the last century. Recently, textiles have faced a new challenge with the advancement of electronics and the internet; textiles are now expected to exhibit additional functionalities besides making people warm and comfortable. For example, the goal of self-power, which is highly desired in electronics, may be easily realized when our clothes are able to convert energy sources such as mechanical energy and solar energy into electric energy; a variety of portable electronic facilities such as mobile phones can be more effectively and conveniently powered if our clothes can store electric energy; it is also promising or required to make electronic devices into textiles for a more efficient use of electricity in many fields, such as displays and sensing. The fact that electricity dominates our life and is everywhere means that the development of smart electronic textiles is important and also has possible practical applications. Indeed, increasing interest has been directed in this direction and clear advancements have been made in recent years.

The variety of applications of smart textiles can be summarized into the following categories. Firstly, it is well recognized that the conventional planar power system cannot effectively meet the requirement of portable and wearable electronic products, so a lot of attention is paid to the incorporation of organic solar cells as well as thermoelectric and piezoelectric devices into textiles to solve the above problem. Taking the organic solar cell as an example, the output powers of a planar solar cell vary at different angles of incident lights, which is a problem for many applications; in contrast, a solar cell textile was developed that showed a stable output power that was independent of the angle of the incident light. Such a property is particularly desired for self-powering applications for various outdoor activities and wireless electronics. Secondly, to more effectively take advantage of the electricity, electrochemically storage devices, including both lithium ion batteries and supercapacitors, have been fabricated into textiles. These devices displayed high electrochemical performances, particularly, as flexible powering systems. Thirdly, a variety of powered facilities such as chromatic and actuating devices have been incorporated into textiles and display high performances. Recently, some attempts have also been made to integrate the above functionalities into electronic textiles.

The textile structure offers unique and promising advantages over conventionally bulky or planar structures. The bulky electronic devices are generally rigid, and the planar electronic devices can be made into thin films which are flexible, but they generally deform on bending along one dimension and often fail under twisting or other severe deformations. In contrast, similar to clothes, a smart textile is typically composed of fibers that can effectively accommodate severe and complex deformations with high stability. The smart textiles are also soft and may be closely contacted onto curved surfaces, which is challenging for their bulky and planar counterparts. This property is critical for wearable applications. In addition, the smart textiles have a lower weight, which is important in microelectronics. Furthermore, the smart textiles are breathable due to the voids formed on assembling the fibers.

Different functional materials have been designed to have different functionalities. For example, photoactive materials were incorporated into fiber or textile electrodes to fabricate solar cells to generate electricity, electrochemically active materials were introduced to obtain energy storage devices for storage of electricity, sensing materials were incorporated into composites to generate color or shape changes through

[*] Dr. W. Weng,[+] P. Chen,[+] S. He, Dr. X. Sun, Prof. H. Peng
State Key Laboratory of Molecular Engineering of Polymers, Collaborative Innovation Center of Polymers and Polymer Composite Materials, Department of Macromolecular Science, and Laboratory of Advanced Materials, Fudan University
Shanghai 200438 (China)
E-mail: sunxm@fudan.edu.cn
penghs@fudan.edu.cn
Prof. H. Peng
State Key Laboratory for Modification of Chemical Fibers and Polymer Materials, Donghua University
Shanghai 201620 (China)
[+] These authors contribute equally to this work.

the use of electricity, and the combination of several materials may produce multiple functionalities.

This Review thus describes smart electronic textiles with a focus on the advancement of functional materials. We examine systems for generating electricity, energy storage, as well as chromatic and deformable devices for an effective use of electricity. The integration of different functionalities is highlighted to reflect a mainstream direction in electronic textiles. The current difficulties are finally summarized to shed light on future study.

2. Electricity-Generating Textiles

Electronic devices are all powered by electricity. We begin our discussion with textiles that can convert other energy source into electric energy. The most accessible forms of energy from the environment include light as well as thermal and mechanical energy. Among them, sunlight, the ambient temperature fluctuation/gradient, and human motion are considered to be abundant sources of energy harvesting that can be converted into electric energy through photovoltaic, thermoelectric, and piezoelectric effects, respectively.[1,2] They have been investigated intensively and are discussed to highlight the main achievements.

2.1. Conversion from Light Energy

The photovoltaic effect generates electricity in a device upon exposure to light, and has been studied for decades. The electrons in the valence band absorb light energy, become excited, and jump to the conduction band to become free. The excited electrons diffuse to reach a junction where they are transported into different materials by a built-in potential to produce electric currents.[3] Solar cells generally demonstrate the above process. Although a variety of solar cells are planar, third-generation solar cells including dye-sensitized solar cells (DSSCs), polymer solar cells, and perovskite solar cells have been incorporated into photovoltaic textiles, as the photoactive materials could be processed through solution methods. Typically, the third-generation solar cells are first fabricated onto fiber substrates, and the fiber-shaped solar cells are then woven into photovoltaic textiles.[4]

2.1.1. Fiber-Shaped Solar Cells

Two main architectures exist in fiber-shaped solar cells: twisted and coaxial structures. In the case of the twisted structure, the photoactive materials are coated onto a fiber electrode and then twisted with another fiber electrode (Figure 1 a,b). For the coaxial structure, a thin layer of electrode material is deposited onto a fiber electrode coated with a photoactive material (Figure 1 c). The twisted structure is more compatible with continuous production and has been

Wei Weng is currently a postdoctoral fellow at the Department of Macromolecular Science and Laboratory of Advanced Materials at Fudan University. He received his BE in Materials Science and Engineering in 2005 and PhD in Materials Science in 2011, both at Shanghai Jiao Tong University. His research focuses on nanomaterials and high-performance composites mainly for energy storage devices and aerospace applications.

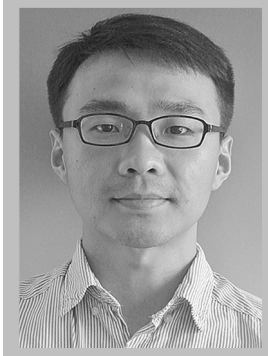

Peining Chen is currently carrying out PhD research at the Department of Macromolecular Science and Laboratory of Advanced Materials at Fudan University. He received his MS in Polymer Chemistry and Physics from Sun Yat-Sen University in 2012 and BE in Light Chemical Engineering from Sichuan University in 2010. His work focuses on actuating and sensing materials/devices.

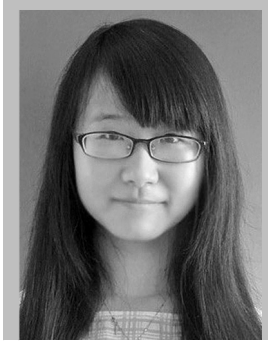

Sisi He received her BS in Material Science and Engineering from Northeastern University in 2011, and MS in Material Science and Engineering from Tianjin University in 2014. She is currently carrying out PhD research in Macromolecular Chemistry and Physics at Fudan University. Her work focuses on the use of aligned carbon nanotube materials in responsive and energy devices.

Xuemei Sun is currently a postdoctoral fellow at the Laboratory of Advanced Materials at Fudan University. She received her BE in Polymer Materials and Engineering from East China University of Science and Technology in 2008 and PhD in Macromolecular Chemistry and Physics at Fudan University in 2013. Her work centers on responsive polymer/carbon nanotube composite materials.

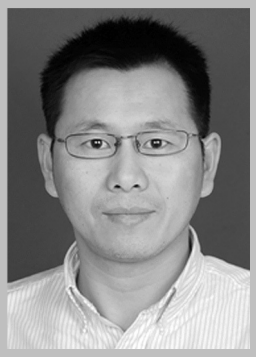

Huisheng Peng is currently a professor at the Department of Macromolecular Science and Laboratory of Advanced Materials at Fudan University. He received his BE in Polymer Materials at Donghua University in China in 1999, MS in Macromolecular Chemistry and Physics at Fudan University in China in 2003, and PhD in Chemical Engineering at Tulane University in USA in 2006. He then worked at Los Alamos National Laboratory before joining Fudan University in 2008. His research centers on the synthesis of aligned carbon nanotube/polymer composite materials and their applications in energy.

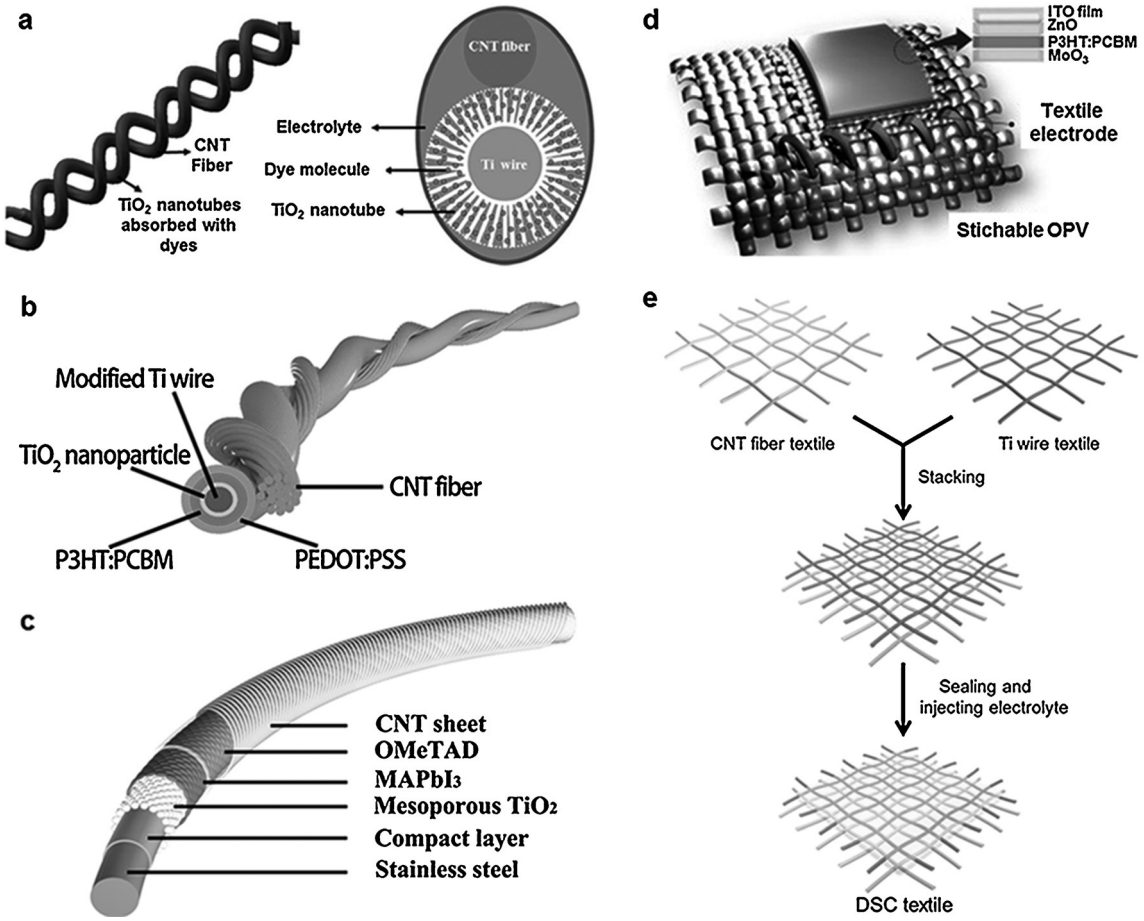

Figure 1. Fiber- and textile-shaped solar cells. a) Twisted fiber-shaped dye-sensitized solar cell based on a Ti wire and a CNT fiber. b) Twisted fiber-shaped polymer solar cell. c) Coaxial fiber-shaped perovskite solar cell. $MAPbI_3 = CH_3NH_3PbI_3$, OMeTAD = 2,2′,7,7′-tetrakis(*N*,*N*-di-*para*-methoxyphenylamine)-9,9-spirobifluorene. d) Concept of a stichable organic photovoltaic cell on a textile electrode. e) Fabrication of a dye-sensitized solar-cell textile based on CNT fiber and Ti wire textiles. Reproduced from Refs. [7, 14, 16, 21, 26], with permission. Copyright 2012 Wiley-VCH; 2014 Wiley-VCH; 2014 Wiley-VCH; 2014 Elsevier; 2014 Wiley-VCH.

studied the most in recent years, while the coaxial structure has been mostly explored as an attempt to develop new photovoltaic devices that mimic the layered design of the conventional planar structure.

A variety of materials have been incorporated into the fiber electrodes. In the early days, metal wires were mostly explored as fiber electrodes because of their high electrical conductivity and low cost.[5] For example, a stainless-steel wire was coated with TiO_2 nanoparticles to form a working electrode and then twisted with a platinum wire as the counter electrode to produce a fiber-shaped DSSC.[6] However, the coated TiO_2 nanoparticles peeled off easily and cracked into patches, which greatly decreased the power conversion efficiency, particularly under deformation. To this end, aligned TiO_2 nanotubes were directly grown onto and more stably adhered to the titanium wire (Figure 1 a).[7] However, when the two metal wires were twisted together, gaps existed between them, which resulted in low efficiencies and poor stabilities. Therefore, flexible polymer fibers were used instead of one metal electrode, such as platinum wire,[8] but the low electrical conductivity from the polymer-based fiber electrode greatly decreased the efficiency. Recently, increasing interest has been paid to spinning carbon nanomaterials, including carbon nanotube (CNT) and graphene, into fibers that simultaneously display high electrical conductivity, tensile strength, and electrocatalytic activity.[7,9] The first fiber-shaped DSSCs twisted from two aligned CNT fibers displayed a relatively low efficiency of 2.94%.[10] The efficiency was recently enhanced to 8.36% after modifications by growing aligned TiO_2 nanotubes on the Ti wire as a working electrode and coating platinum nanoparticles on the CNT/graphene hybrid fiber as the counter electrode.[11] The aligned structure of the TiO_2 nanotubes, the high loading of platinum nanoparticles, and the interaction of the CNTs and graphene in the carbon nanomaterial fiber contribute to the much improved photovoltaic performance.

The fiber-shaped DSSCs were typically made from liquid electrolytes, which may leak and decrease the efficiency and stability. To this end, quasi-solid-state electrolytes were used in recent years to replace the liquid electrolytes to increase the stability, but the efficiency was greatly decreased to 3.51%.[12] To further increase the stability and efficiency, all-solid-state polymer solar cells have also been incorporated into fibers (Figure 1 b).[13,14] Typically, a fiber-shaped polymer

solar cell was fabricated by twisting a photoactive polymer-coated core electrode through a continuous solution process with another electrode, and an efficiency of 3.8% was achieved.[15] In addition, the efficiency remained almost unchanged over time and under bending. Nevertheless, the efficiency of the fiber-shaped polymer solar cell needs to be further enhanced for practical applications, and a lot of effort is currently being made to develop new fiber electrodes and optimize the cell structure.

Recently, the perovskite solar cell rose as a new star of photovoltaic devices because of its much higher efficiency than both DSSCs and polymer solar cells. Naturally, some attempts were also made to fabricate the perovskite solar cell into a fiber shape. For example, a coaxial fiber-shaped perovskite solar cell was achieved by sequentially coating a compact layer, a mesoporous TiO_2 layer, and a perovskite $CH_3NH_3PbI_3$ sensitizer onto a stainless steel wire electrode, followed by coating with the hole-transport material and winding around a transparent CNT sheet as the cathode (Figure 1c).[16] An efficiency of 3.3% was produced, and this value was expected to increase after optimization, such as by the introduction of new electrode materials and using an annealing treatment during fabrication.

Besides designing new photoactive layers and achieving high efficiencies, stretchable fiber-shaped solar cells have also been proposed to expand their application scope. A typical stretchable fiber-shaped DSSC was fabricated by twisting a modified Ti wire onto a rubber fiber wound with aligned CNT sheets, followed by coating with photoactive materials.[17] It produced an efficiency of 7.13%, which was stable on repeatedly stretching by 30%. The stability and durability could be further improved by replacing the liquid electrolyte with a polymer/ionic liquid gel, which could effectively work even at 300°C but with a decreased efficiency.[18] A typical stretchable fiber-shaped polymer solar cell was also obtained by winding an aligned CNT sheet onto a spring-like modified Ti wire electrode that was attached to an elastic fiber substrate, and with a layer of photoactive materials coated on the Ti wire.[19] Although it exhibited a low efficiency of 1.23%, the efficiency varied by less than 10% after bending 1000 times and on stretching over 30%. These stretchable fiber-shaped solar cells can be further woven into stretchable photovoltaic textiles for wearable and portable applications.

2.1.2. Textile-Shaped Solar Cells

Photovoltaic textiles can either be woven from fiber-shaped solar cells or they can also be directly fabricated from textile substrates based on polymer fibers. As the polymer textiles demonstrate low electrical conductivities or are even insulating, a conductive layer of metals, such as silver and gold, or carbon nanomaterials is typically required and coated on them prior to the deposition of the photoactive materials.[20–22] For example, when a hole transporting layer of poly(3,4-ethylenedioxythiophene):poly(styrene sulfonate) (PEDOT:PSS), a photoactive layer, and a transparent LiF/Al electrode were sequentially deposited onto a silver-modified textile, the resulting polymer solar cell displayed an efficiency of 0.33%.[20] The efficiency was enhanced to 1.8% after optimization, such as by using MoO_3 as the hole transport layer, ZnO as the electron transport layer, and indium-tin oxide as the electrode (Figure 1d).[21] Recently, a reduced graphene oxide was coated on a cotton fabric to act as the counter electrode in a DSSC that achieved a higher efficiency of 2.52%.[22]

A variety of metal wires can be woven into a mesh to generate a textile electrode with much improved electrical conductivity compared to the polymer textile. For example, aligned TiO_2 nanotubes were perpendicularly grown on a Ti textile as the working electrode in a polymer solar cell,[23] and ZnO nanorods were perpendicularly grown on a textile based on a stainless steel wire to act as the working electrode in a DSSC.[24] A slightly enhanced efficiency of 2.63% was obtained for a typical DSSC textile fabricated from the TiO_2-coated metal, carbon yarn coated with platinum nanoparticles, and an acetonitrile-based electrolyte.[25] However, platinum nanoparticles needed to be loaded on the conductive textile to improve the catalytic activity of the counter electrode in the DSSC textile.[24,25]

Aligned CNT fibers have been widely studied because of their combined high electrical conductivity, tensile strength, and catalytic activity. They have also been woven into textile electrodes, which inherited the above desirable properties. Indeed, when a counter electrode textile made from CNT fibers was stacked onto a Ti working electrode textile with perpendicularly grown TiO_2 nanotubes, the resulting textile-shaped DSSC exhibited a much improved efficiency of 3.67%, with the high efficiency also preserved during bending (Figure 1e).[26] Thus, as expected, these photovoltaic textiles were flexible.

To summarize, these organic solar cells have an elegant structure with a sequential order of a working electrode, an electron transport layer, an electron-activated layer, a hole-transport layer, and a counter electrode, with the materials having suitable energy bands. Although the newly developed perovskite solar cells exhibit high power conversion efficiencies, their performances are not good in fibers or textile shapes because the morphologies of these functional layers are difficult to control on nonplanar substrates. Polymer solar cells are easy to adapt to the fiber or textile format, but their performances are poor. For the DSSCs, the power conversion efficiencies in fiber materials have been enhanced to above 9%. However, the use of a liquid electrolyte hinders their applications. It is difficult and complex to seal a fiber device, and possible leakage of the liquid electrolyte also brings a severe safety problem, particularly, for wearable applications.

2.2. Conversion from Thermal Energy

The thermoelectric effect is generally used to convert thermal energy into electric energy. The most explored thermoelectric devices convert temperature gradients (dT/dx) to electric energy through the Seebeck effect, while the less explored pyroelectric effect generates electricity from temperature fluctuations (dT/dt) as a result of thermal

diffusion. A high temperature gradient or fluctuation is preferred,[27] and thus thermoelectric devices are rarely used in wearable electronics. On the other hand, it would be adventitious if the heat from the human body could be used to generate electricity effectively.[28] In the following section, some prototypes that may be extended to power textiles are presented.

2.2.1. Thermoelectricity

A thermoelectric power generator has a simpler structure than a solar cell. It is basically composed of thermoelectric material and positive/negative electrodes. There are two methods to fabricate thermoelectric textiles, either conventional brittle thermoelectric materials are coated on flexible substrates or flexible thermoelectric materials are used directly.

In a typical fabrication based on conventional thermoelectric materials, n-type Bi_2Te_3 discs and p-type Sb_2Te_3 discs were first printed alternately on a glass fabric (Figure 2a). Cu film embedded in the polydimethylsiloxane elastomer was used for the connection. The resulting device with eight thermocouples exhibited a high output power density of 3.8 mW cm^{-2} at $\Delta T = 50$ K.[29] However, conventional thermoelectric materials such as Bi_2Te_3 and PbTe are brittle, toxic, and heavy.[30–32]

Novel flexible CNT/polymer fabrics were then developed to harvest thermoelectricity.[33] Both p- and n-type fabrics have been realized by functionalizing the junctions in CNT mats. The thermoelectric modules were made by alternately and electrically connecting p- and n-type CNT films with Al foils in series by using a silver adhesive, and p-type and n-type films were thermally stacked in parallel. The output thermoelectric voltage reached 9.3 mV K^{-1} when eight modules were electrically connected in series. This thermoelectric device produced an output voltage of 150 mV. A simpler thermoelectric fabric was further developed from a multilayered CNT/poly(vinylidene fluoride) (PVDF) composite.[32] It was fabricated by alternately stacking n- and p-type conductive composite layers separated by an insulating bare PVDF layer (Figure 2b). A thermoelectric voltage of about 240 μV K^{-1} was generated with 30 conducting layers.

Some further studies investigated the performance of thermopiles directly attached to the skin or integrated into various garments.[34] The clothes that covered thermopiles were found not to appreciably lower the power generation. Generated powers ranged from 5 to 0.5 mW at ambient temperatures of 15 to 27 °C. More studies are required to increase the power output and other properties.

2.2.2. Pyroelectricity

A pyroelectric power generator has a similar structure as a thermoelectric generator. However, the active component is the pyroelectric material, and its function is based on thermal diffusion. There are two main strategies to increase the pyroelectric current: increasing dT/dt and increasing the pyroelectric coefficient of the active material.[35] In the case of a flexible pyroelectric generator, the performance can generally be improved by increasing dT/dt through structural

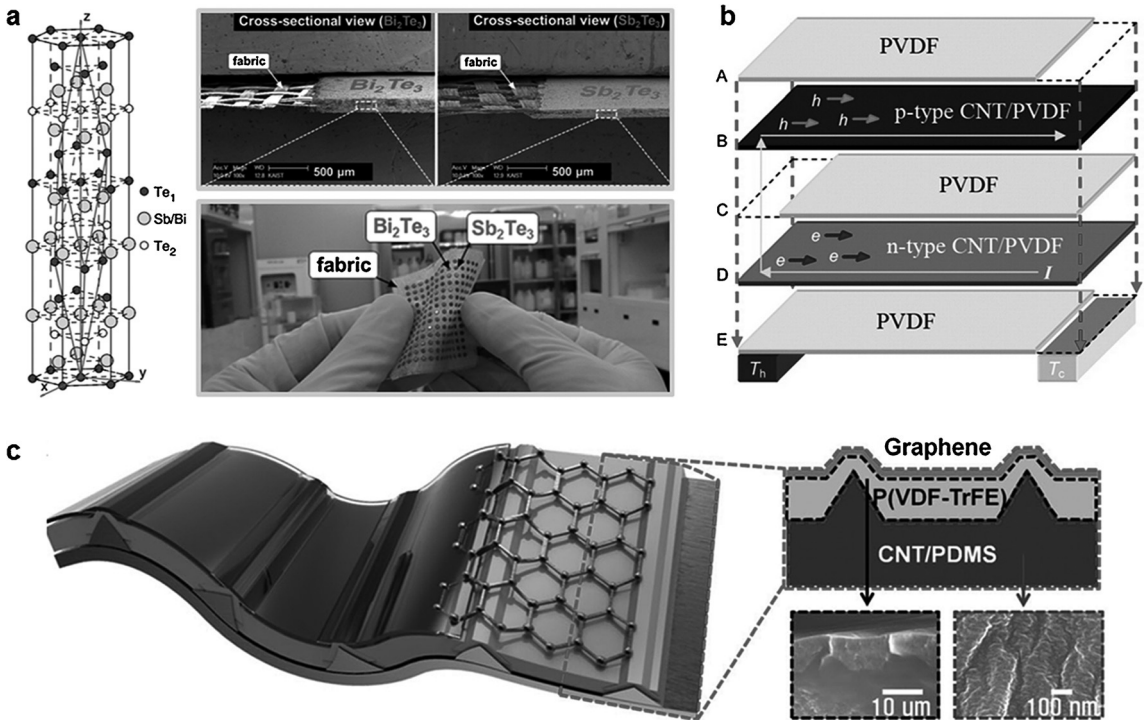

Figure 2. a) Crystal structure of Bi_2Te_3 and Sb_2Te_3, SEM images of the screen-printed thick Bi_2Te_3 and Sb_2Te_3 films on a glass fabric, and a photograph of the resulting textile-shaped thermoelectric device. b) A flexible thermoelectric device based on a multilayered structure composed of PVDF and CNT/PVDF films. c) Schematic illustration of a highly stretchable piezoelectric nanogenerator with a micropatterned structure. Reproduced from Refs. [29, 32, 36] with permission. Copyright 2014 RSC; 2012 ACS; 2014 Wiley-VCH.

optimization since there is only a limited source of flexible pyroelectric materials.

It is recognized that replacement of a fully covered electrode with a partially covered electrode increases the thermal diffusion because of the high radiation absorption coefficient of the pyroelectric material. Therefore, micropatterned and unpatterned Ti/Al electrodes were deposited on two sides of a PVDF film to fabricate a pyroelectric device.[35] It showed 66.9 $\mu J\,cm^{-3}$ per cycle at an oscillation temperature of 2.8 °C. The open-circuit voltage and short-circuit current were improved by 380 % and 420 %, respectively, for an electrode with a covered area of 45 % compared to a fully covered one. A stretchable pyroelectric generator based on the micropatterned structure was also developed to more effectively accommodate the deformation (Figure 2c).[36]

Thermoelectric and pyroelectric generators have similar and relatively simple configurations that are composed of one functional layer connected to positive and negative electrodes. For practical applications, thermoelectric generators are more suitable for wearable devices than pyroelectric ones because a temperature gradient is generally produced between the human body and the environment. However, a large number is needed to generate a large temperature gradient with a number of units connected in parallel/series. It also remains difficult to find high-performance and flexible thermoelectric materials.

2.3. Conversion from Mechanical Energy

The piezoelectric effect has mostly been investigated in regard to converting mechanical energy into electric energy. Of decisive importance for the piezoelectric effect is the polarization change in the piezoelectric material under a mechanical stress. The change in polarization appears as a variation in the surface charge density. Energy harvesting devices based on the piezoelectric effect have been investigated for decades.[36–43] They are simply constructed on piezoelectric materials and positive/negative electrodes. Previous studies showed that a high piezoelectric coefficient of the active material and the connection (in parallel and series) are two major factors to effectively increase the output.[40,44–46] Commonly, alternating current/voltage outputs are obtained in a cycle consisting of exerting and releasing stress. In 2008, a fiber-shaped piezoelectric nanogenerator (PENG) gave a direct output.[40] Thereafter, fiber- and textile-shaped PENGs started to attract increasing attention.

2.3.1. Fiber-Shaped Piezoelectric Generators

The above-mentioned fiber-shaped PENG was fabricated by radially growing piezoelectric ZnO nanowires around Kevlar fibers (Figure 3a).[40] The tips of nanowires were separated from each other as a consequence of their small tilting angles, but their bottom ends were tightly connected. The space between the nanowires was on the order of hundreds of nanometers, which was large enough for them to be bent to generate a piezoelectric potential. Two hybrid fibers were twisted to form the PENG, which generated electricity on pulling/releasing the string. An output power density of 4–16 mW per square meter was expected if it was woven into a fabric.

A core-sheath structure was developed for a fiber-shaped PENG that worked under sinusoidal axial tension.[47] The sheath was made of PVDF, while a conductive composite of carbon black and high-density polyethylene was used for the core. A bundle of 24 PENG fibers produced a voltage output of 4 V when undergoing a sinusoidal axial tension of 0.07 % strain. The average power was evaluated to be 15 nW at a length of 25 mm.

To improve the performance, a hybrid fiber-shaped PENG was fabricated by coating a PVDF layer onto the ZnO nanowire (Figure 3b).[45] Here, PVDF acted as both the protective and piezoelectric material. An additional Au film was deposited on half of the outermost surface to serve as the other electrode for the polarization of PVDF. Afterwards, the PVDF was polarized along the direction of the *c*-axis of the ZnO nanowire array to align the piezoelectric dipoles in the active piezoelectric layer. By attaching a hybrid fiber-shaped PENG with a length of 2 cm on a human arm that folded and released through an angle of 90°, the output voltage, current density, and power density reached 0.1 V, 10 $nA\,cm^{-2}$, and 16 $\mu W\,cm^{-3}$, respectively.

PENG could be further assembled with other types of nanogenerators such as a triboelectric nanogenerator for more-efficient collection of mechanical energy.[48] For a typical fiber-shaped generator, the triboelectric nanogenerator was positioned in the core and covered with PENG to form a coaxial structure. The PENG not only enhanced the collection efficiency of the mechanical energy but also generated an electric output when the triboelectric nanogenerator was not working. The power densities for the triboelectric and piezoelectric nanogenerators reached 42.6 and 10.2 $mW\,m^{-2}$, respectively.

2.3.2. Textile-Shaped Piezoelectric Generators

Piezoelectric textiles were realized by using fibers coated with ZnO nanwires.[49] They were composed of two kinds of fibers that were interwoven with each other, one fiber grown with ZnO nanwires and the other sequentially grown with ZnO nanowires and coated with palladium. Depending on the coupled piezoelectric and semiconducting properties of the ZnO, it generated electricity when driven by a tiny external mechanical force such as wind and sound. The performance of the piezoelectric textile was relatively poor, with an open-circuit voltage of 3 mV and a short-circuit current of 17 pA. To enhance the performance, piezoelectric textiles were fabricated by weaving flexible piezoelectric PVDF fibers.[50] PVDF filaments were prepared by a spinning method along with a polarization treatment. The piezoelectric PVDF contained a high portion of the β-phase (nearly 80 %), which was favorable for enhancing the piezoelectric effect. The PVDF filaments were then woven into a three-dimensional spacer fabric, which was sandwiched between silver-coated polyamide layers that acted as the top and bottom electrodes to produce a piezoelectric textile (Figure 3c). Power densities of

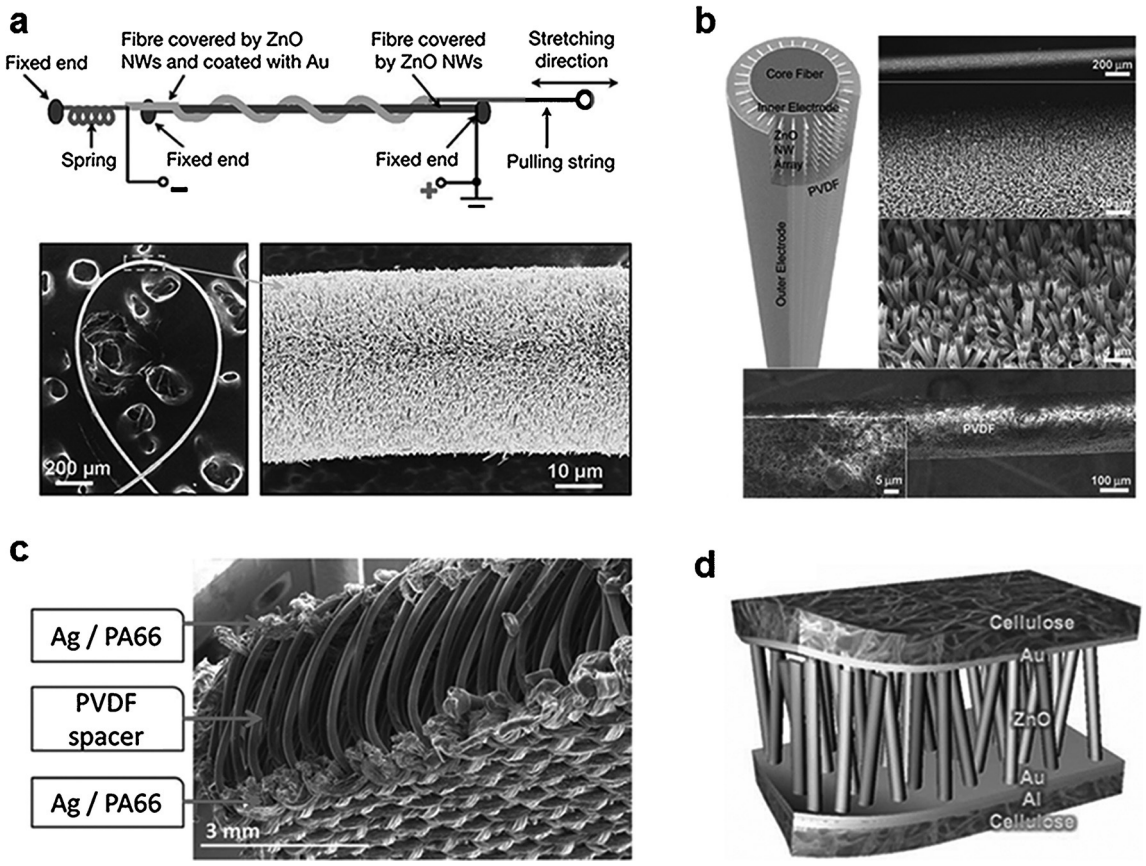

Figure 3. Fiber- and textile-shaped piezoelectric nanogenerators. a) Fiber-shaped piezoelectric nanogenerator based on two fibers coated with ZnO nanowires. b) Hybrid fiber-shaped piezoelectric nanogenerator based on ZnO nanowires and PVDF-coated fibers. c) Cross-sectional SEM image of piezoelectric textiles with a three-dimensional spacer. d) Schematic diagram of an integrated paper piezoelectric nanogenerator with ZnO nanorods on foldable cellulose paper. Reproduced from Refs. [40, 45, 50, 53] with permission. Copyright 2008 Nature; 2012 Wiley-VCH; 2014 RSC; 2011 Wiley-VCH.

1.10–5.10 $\mu W\,cm^{-2}$ were generated under pressures of 0.02–0.10 MPa.

Besides weaving piezoelectric fibers into textiles, piezoelectric textiles can also be fabricated by directly growing piezoelectric materials onto textile electrodes. A silver-coated cotton textile was developed as an electrode for the growth of ZnO nanorods to produce a PENG.[51] An average output voltage of 9–9.5 mV was obtained. This energy-harvesting textile was further improved by growing ZnO nanoneedles on a commercial conductive textile.[52] The piezoelectric potential was over 45 mV and the corresponding current was greater than 150 μA. Paper was also studied as a promising substrate for the PENG, typically with a sandwich structure (Figure 3d), that is, a metal-coated cellulose paper at the bottom, ZnO nanorods in the middle, and Au-coated cellulose paper at the top.[53] It generated electricity under a pushing force perpendicular to the PENG, with an output current density of approximately 2.0 $\mu A\,cm^{-2}$.

To summarize, although all piezoelectric materials can generate electric outputs, only ZnO and PVDF prevail in fiber- and textile-shaped piezoelectric nanogenerators. PVDF itself can be made into flexible fibers, but the performance needs to be greatly improved for real applications. Although ZnO has a lower piezoelectric constant than the other piezoelectric ceramic materials such as $PbTiO_3$ and $PbZrTiO_3$, it is much safer. Besides, the synthesis of ZnO is well understood, both with various morphologies and on different substrates. Furthermore, ZnO can simultaneously possess piezoelectric and semiconducting properties, thereby resulting in a direct current/voltage output.

3. Textiles for Electricity Storage

Besides generating electricity, it is also important to store electricity for effective use. Thus, energy-storage textiles are required for wearable electronics. Lithium ion batteries and supercapacitors represent two main formats for storing electricity as a result of their high energy and high power densities, respectively, and both of them have been incorporated into energy-storage textiles in recent years.[54–56]

3.1. Lithium Ion Batteries

A lithium ion battery consists of a negative electrode, a positive electrode, and an electrolyte. For a typical working process, lithium ions move from the negative electrode to the

positive electrode during discharging and in the reverse direction during charging. An intercalated lithium compound is used for one electrode in chargeable lithium ion batteries, whereas metallic lithium is used in non-rechargeable lithium batteries. The electrolyte allows ionic transport between the negative and positive electrodes. Some basic information and preparation process on how to make conventional rigid batteries are first introduced. Both electrodes are composed of active material, conductive additive, and binder. Active materials in the positive electrode typically include lithium salts, such as $LiCoO_2$, $LiMn_2O_4$, and $LiFePO_4$.[57–59] Active materials in the negative electrode are classified into carbonaceous materials, metals/alloys, and oxides/sulfides (e.g. $Li_4Ti_5O_{12}$).[60–62] The binder is made of thermoplastic polymers, and conductive additives are made of carbonaceous materials such as carbon black, CNTs, and graphene. To prepare an electrode, a slurry of active material, binder, and conductive additive is formed first and then cast onto a current collector (usually Cu for the negative electrode and Al for the positive electrode). This preparation process is compatible with conventional rigid planar batteries but becomes difficult for flexible battery fibers and textiles, as rigid current collectors and electrodes are typically used.

3.1.1. *Fiber-Shaped Lithium Ion Batteries*

Similar to the solar cells discussed above, two main architectures exist for fiber-shaped lithium ion batteries, namely, coaxial and twisted structures. In both cases, the fiber electrode plays a critical role on the performance of the fiber-shaped battery. For example, a cable-type battery with a coaxial structure was fabricated from a hollow multihelix electrode that consisted of several electrode strands coiled into a hollow-spiral core and surrounded by a tubular outer electrode.[63] The cable-type battery could be cycled in a voltage window of 2.5 to 4.2 V and had a linear specific capacity of 1 $mAh\,cm^{-1}$. However, these cable-type batteries had diameters of millimeters to centimeters and were difficult to weave into flexible textiles. Furthermore, the use of a metal current collector greatly increased the weight and volume of the battery and resulted in low flexibility.

A variety of aligned CNT-based fibers such as CNT/MnO_2 and CNT/silicon composite fibers were then developed to replace the metal materials. As previously mentioned, aligned CNT fibers display both high electrical conductivity and tensile strength, and they can be used to coat metal oxide and silicon on the surfaces of CNTs by electrochemical deposition and electron beam evaporation, respectively.[58,64,65] Metal oxide and silicon were widely investigated because of their high specific capacities, and the resulting composite fibers were expected to demonstrate high electrochemical performances. In addition, the aligned CNT composite fibers were conductive, so no binder was required in the fiber electrode. A half-cell assembled from a CNT/Si composite fiber by using a lithium wire as the counter electrode showed a specific capacity of nearly 1600 $mAh\,g^{-1}$ at a current density of 1 $A\,g^{-1}$.[65] To more effectively restrict the volume expansion of the Si nanoparticles during charging and discharging, another aligned CNT sheet was coated on the outer surface of the CNT composite fiber. A fiber-shaped full battery was then fabricated by sequentially winding the CNT/$LiMn_2O_4$ and CNT-Si/CNT composite fibers onto a cotton fiber, with the two composite fiber electrodes separated by a gel electrolyte.[66] The battery demonstrated a high linear energy density of 0.75 $mWh\,cm^{-2}$.

To expand the application scope of the fiber-shaped batteries, it is necessary for them to be both elastic and flexible so that they can work effectively in wearable electronics during a stretching movement. A stretchable fiber-shaped battery can be produced if an elastic polymer fiber is used as the substrate instead of a cotton fiber. Flexible fiber-shaped batteries were first fabricated by pairing aligned CNT/$Li_4Ti_5O_{12}$ and CNT/$LiMn_2O_4$ composite fibers as the anode and cathode, respectively (Figure 4a).[58] The cathode and anode fibers were assembled in parallel and wrapped onto the heat-shrinkable tube (Figure 4b), followed by coating a thin layer of gel electrolyte and inserting into another heat-shrinkable tube. As no extra current collectors and binders were required during the fabrication, the resulting battery was stretchable as a result of the wound structure and could be stretched up to 100%. After optimization, a super-stretchy battery was prepared that maintained a specific capacity of 88% at a high strain of 600%.[67] However, the elastic substrate increased the weight and volume as well as decreasing the specific capacity to 0.01 $mAh\,cm^{-1}$. In addition, the low tensile strength and low thermal stability of the

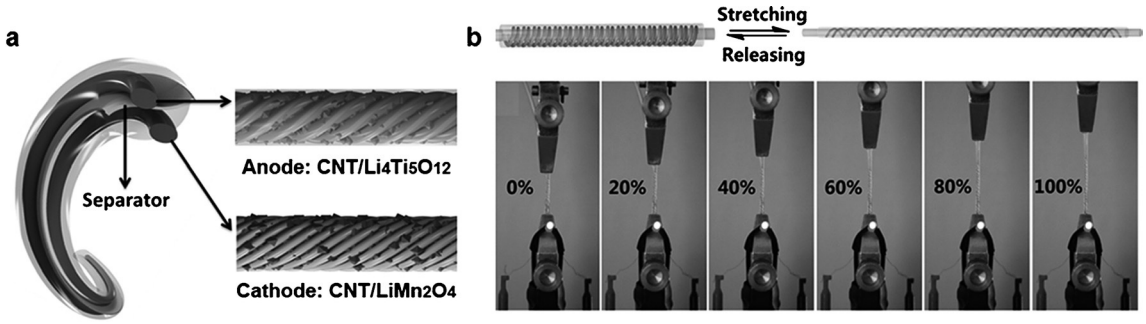

Figure 4. a) Structure of a flexible fiber-shaped lithium ion battery based on aligned CNT/$Li_4Ti_5O_{12}$ and CNT/$LiMn_2O_4$ composite fibers as the anode and cathode, respectively. b) Stretchable fiber-shaped lithium ion battery on an elastic polymer fiber substrate that powers a light-emitting diode as the strain increases. Reproduced from Ref. [58] with permission. Copyright 2014 Wiley-VCH.

elastic polymer limited their applications. Therefore, it was necessary to further realize stretchable fiber-shaped batteries without using elastic substrates.

Inspired by the stretchable spring, a battery can be made into spring structures that are stretchable even if the fiber-shaped battery itself is rigid. An aligned CNT spring was prepared by over-twisting several CNT fibers together and could then be stretched by 100%.[68] Similarly, active $Li_4Ti_5O_{12}$ and $LiMn_2O_4$ nanoparticles could be incorporated into the CNT fibers, followed by over-twisting into a spring. After being impregnated with the gel electrolyte, which also served as the separator, a stretchable battery was then produced with an average discharge voltage plateau of 2.5 V. It exhibited a much higher reversible specific capacity of 2.2 $mAh\,m^{-1}$ than one based on an elastic polymer fiber substrate. The specific capacities were maintained at 85% even at a strain of 100%.

As expected, the fiber-shaped batteries could be further woven into energy-storage textiles. For example, the textiles made from fiber-shaped batteries on cotton fibers showed an energy density of 4.5 $mWh\,cm^{-2}$.[66] Although some battery textile models have been demonstrated, it is not yet possible to continuously produce effective energy-storage textiles from fiber-shaped batteries. A main reason for this is that the length of the current fiber-shaped battery is limited to millimeters/centimeters. Some general and efficient fabrication methods are highly desired to make fiber-shaped batteries on a large scale.

3.1.2. Textile-Shaped Lithium Ion Batteries

Lithium ion battery textiles can also be made directly from textile electrodes, for example, from polymer textiles coated with conductive material. For example, Ni was coated on polyester textiles as electrodes, followed by deposition of a slurry composed of active materials, denka black, and polyurethane binder; commercial $LiFePO_4$ and $Li_4Ti_5O_{12}$ were used for the cathode and anode, respectively.[69] The battery textile worked in a voltage window of 0.6–2.4 V and demonstrated a specific capacity of 100 $mAh\,g^{-1}$ at 0.5 C. Compared with the insulating polymer textiles that require further deposition of conductive layers, conductive textiles such as carbon cloths are prevalent. A variety of active materials, such as $ZnCo_2O_4$ nanowire arrays,[70] WO_3@SnO_2 core-shell nanowire arrays,[71] Fe_2N nanoparticles,[72] and aligned $Ca_2Ge_7O_{16}$ nanowire arrays,[73] were deposited on these conductive textiles. The electrochemical performances of these battery textiles were greatly increased. A high rate capability of 103 $mAh\,g^{-1}$ at 90 C and a good cyclic stability with 5.3% loss in specific capacity after 200 cycles at a rate of 10 C was achieved with the carbon textile electrode.[74]

3.2. Supercapacitors

In contrast to batteries with high energy densities, supercapacitors have been widely investigated in regard to high power densities. Similar to lithium ion batteries, supercapacitors have a structure with the electrolyte sandwiched between two electrodes. They can be categorized as electrostatic double-layer capacitors and pseudocapacitors according to the energy-storage mechanism. An electrostatic double-layer capacitor is typically made from carbon electrodes and realizes charge separation at the interface between the electrode and electrolyte.[75–77] A pseudocapacitor is generally fabricated from metal oxide or conducting polymer electrodes and uses redox reactions to store energy.[77,78] Both types of capacitor have been made into fibers and textiles.

3.2.1. Fiber-Shaped Supercapacitors

There are many more reports on fiber-shaped supercapacitors than lithium ion batteries, possibly because the fabrication of the former is much easier. Three fiber electrodes, namely, polymer fibers, metal fibers, and carbonaceous fibers have been mainly explored to produce fiber-shaped supercapacitors.[68,79–93] Similar to the other fiber-shaped electronic devices, the fiber-shaped supercapacitors can have coaxial and twisted structures.

A cable-type supercapacitor was fabricated based on three-dimensional nanostructures made from polypyrrole, MnO_2, and CNT-cotton thread.[80] It was produced by coating CNTs onto porous cotton threads, followed by electrodepositing MnO_2 and polypyrrole. An energy density of 33 $\mu Wh\,cm^{-2}$ and a power density of 0.67 $mW\,cm^{-2}$ was obtained. In this case, the cotton fiber was insulating and did not contribute to the energy storage, thus decreasing the overall specific capacity. To improve this situation, metal fibers were used as conductive electrodes because of their high electrical conductivities. For example, a coaxial fiber-shaped supercapacitor was fabricated from a steel fiber that was sequentially coated with an ink, gel electrolyte, active carbon, and silver paint.[82] The specific capacitance was calculated to be 3.18 $mF\,cm^{-2}$ or 0.1 $mF\,cm^{-1}$. To further improve the performance, an asymmetric fiber-shaped supercapacitor with a twisted architecture was designed by using Ni/Co_3O_4 nanowires and carbon/graphene fiber electrodes.[91] A high specific capacitance of 2.1 $F\,cm^{-3}$ at a current density of 20 $mA\,cm^{-3}$ was achieved, and the potential window was increased from 0.6 to 1.5 V. The stored energy and delivered power were enhanced by at least 1860%. However, the metal fiber was heavy and also showed limited flexibility.

To this end, carbonaceous fibers were intensively investigated as they are lightweight, more flexible, and more stable than metal wires. Polyelectrolyte-wrapped graphene/CNT fibers were prepared by a coaxial wet-spinning process.[87] A fiber-shaped supercapacitor was produced by twisting two fiber electrodes with a solid electrolyte. It showed both a high specific capacitance of 177 $mF\,cm^{-2}$ and a high energy density of 3.84 $\mu Wh\,cm^{-2}$. Polyaniline could also be incorporated into aligned CNT fibers by electrodeposition to further increase the specific capacitance. Two CNT/polyaniline composite fibers were twisted to produce a fiber-shaped supercapacitor with a specific capacitance of 274 $F\,g^{-1}$ or 263 $mF\,cm^{-1}$ (Figure 5a).[84] Besides the twisted architecture, a coaxial structure was also designed for the fiber-shaped supercapacitor by winding a CNT sheet onto a CNT fiber with a polymer electrolyte sandwiched between them (Figure 5b).[89] It

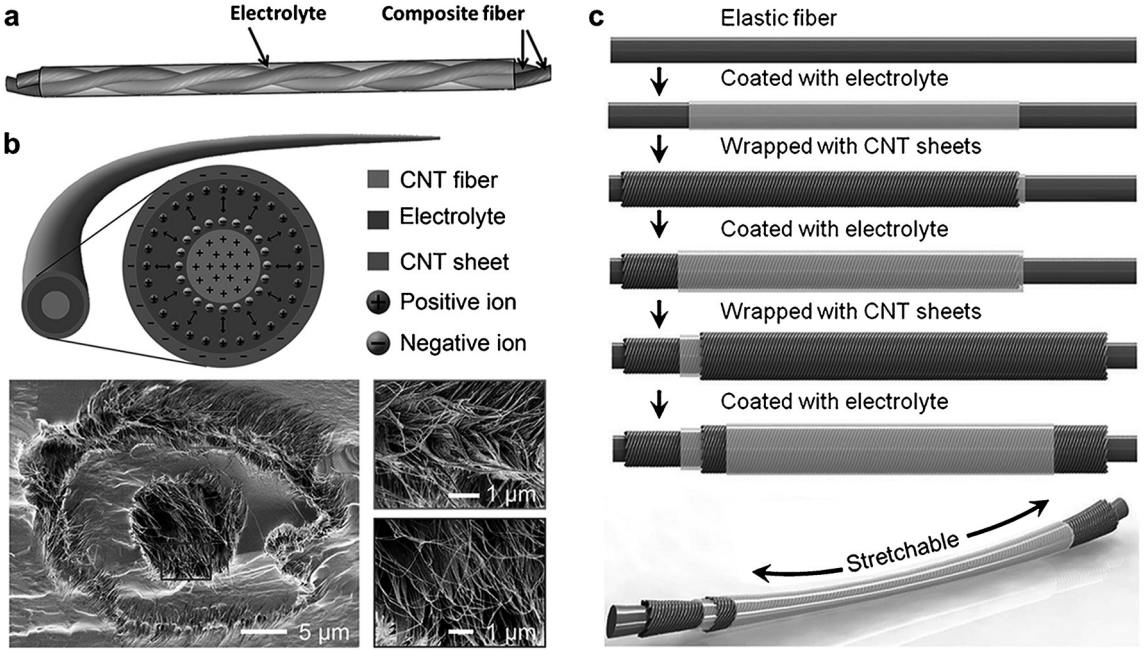

Figure 5. Fiber-shaped supercapacitors. a) Two aligned CNT/polyaniline composite fibers twisted into a supercapacitor. b) Coaxial fiber-shaped supercapacitor based on aligned CNT fibers and sheets. c) Illustration of the fabrication of a stretchable, coaxial fiber-shaped supercapacitor on an elastic polymer fiber substrate. Reproduced from Refs. [84, 89, 94] with permission. Copyright 2013 RSC; 2013 Wiley-VCH; 2013 Wiley-VCH.

showed a specific capacitance of 58 $F g^{-1}$, much higher than the 4.5 $F g^{-1}$ for the fiber-shaped supercapacitor formed by twisting two CNT fibers together. This difference may be explained by the fact that the coaxial structure decreased the contact resistance between the two electrodes.

Besides achieving a high storage capability, increasing effort has recently focused on the incorporation of more functionality into the fiber-shaped supercapacitors. Similar to the elastomeric fiber-shaped lithium ion battery, stretchable fiber-shaped supercapacitors have also been realized on elastic fiber substrates (Figure 5c).[94] An elastic rubber fiber was sequentially coated with a thin layer of poly(vinyl alcohol)/H_3PO_4 gel electrolyte, wound with a CNT sheet as the inner electrode, coated with a second layer of electrolyte, wound with another CNT sheet as the outer electrode, and finally coated with a third layer of the electrolyte. The use of aligned CNT sheets offered high flexibility, tensile strength, electrical conductivity, as well as mechanical and thermal stability simultaneously. The fiber-shaped supercapacitor maintained a specific capacitance of 18 $F g^{-1}$ after stretching 100 times by 75%. After replacement of the rubber fiber with a polydimethylsiloxane fiber and introduction of conducting polymers such as polyaniline, both higher strain and higher specific capacitance were achieved in the fiber-shaped supercapacitor.[92] A specific capacitance of 79.4 $F g^{-1}$ was maintained after stretching 5000 times by 300%.

3.2.2. *Textile-Shaped Supercapacitors*

Fiber-shaped supercapacitors have been widely studied for their ability to be woven into energy-storage textiles that are flexible, stretchable, and smart. Recently, some attempts were also made to produce textile-shaped supercapacitors directly from textile electrodes. Insulating textile substrates are generally prepared by coating a conductive layer on the surface to serve as the electrodes. A cotton textile dip-coated with CNTs displayed an electrical conductivity of 125 $S cm^{-1}$ and a sheet resistance of less than 1 Ωsq^{-1}.[95] The resulting supercapacitor textile showed a capacitance of up to 0.48 $F cm^{-2}$. A higher capacitance of 2.8 $F cm^{-2}$ at a scan rate of 0.05 $mV s^{-1}$ was achieved by incorporation of MnO_2 nanoflowers into the CNT.[96] Similarly, a graphene-coated cotton cloth was used to generate a high-performance supercapacitor textile with a specific capacitance of 81.7 $F g^{-1}$[97].

Compared with the insulating textiles coated with conductive layers, conductive textiles are, by nature, more suitable for textile-shaped supercapacitors. Examples of such textiles are stainless-steel mesh,[98] carbon cloth,[99] and CNT networks.[100–102] For example, an all-solid-state polymer supercapacitor was made from a CNT network electrode.[100] PANI was first uniformly coated onto freestanding CNT networks, and then two CNT/polyaniline composites were coated with a H_2SO_4-poly(vinyl alcohol) electrolyte and pressed together to produce the supercapacitor. The thickness of the entire device was close to that of commercial standard A4 paper. It showed a high specific capacitance of 350 $F g^{-1}$ based on the electrode material, a low leakage current of 17.2 μA, and high cyclic stability. The specific capacitance of the entire device also reached 31.4 $F g^{-1}$.

In summary, gel and solid electrolytes are preferred over liquid electrolytes for both lithium ion batteries and supercapacitors in a wearable fiber- or textile-shaped device. However, the packaging materials are typically constructed to be waterproof and airtight, which is opposite to the

definition of a textile. The applicability of conventional textile processing for the fiber-shaped devices should be carefully investigated but remains unavailable yet.

4. Electriconic Textiles

A variety of electronic devices including displays, light-emitting electrochemical cells, and mechanical actuators have been made into textiles. Some of these electrically driven systems demonstrate high performances that were not possible with their planar counterparts. Three representative functionalities are discussed to highlight the advantages of fiber and textile shapes.

4.1. Electrochromism

Electrochromic materials and devices may demonstrate different and reversible colors in response to the applied voltage or current.[103–105] They are promising for the next generation of wearable displays because of their ability to work on flexible substrates and at low power consumptions. Active materials are typically sandwiched between two planar electrodes and immersed in liquid electrolytes in electrochromic devices. The electrodes are usually composed of transparent rigid glasses coated with conductive indium tin oxide layers, which is incompatible for flexible applications. To this end, flexible conductive electrodes were made by coating or compositing conductive components such as indium tin oxide, silver nanowires, CNTs, graphene, and conducting polymers onto plastic substrates.[106–110] Gel and solid electrolytes were also developed to construct air-operated electrochromic devices.[111] Conducting polymers have been mostly explored as active materials for the flexible electrochromic devices because of their wide color spectrum, good coloration efficiency, low operation voltage, and rapid switching ability. However, the planar shape and airtight structure limit their applications in microelectronics and wearable electronics. Naturally, increasing attention is paid to make electrochromic textiles based on electrical field, the electrothermal effect, and electrochemically induced redox reactions. The electrochromic textiles are produced by weaving electrochromic fibers into textiles, or they can be obtained directly on the conductive textile substrates.

4.1.1. Electrochromic Fibers

Electrochromic fibers were first synthesized from aligned CNTs and conjugated polymers, and they displayed reversible color changes when electric currents were applied (Figure 6a).[112] The aligned CNTs made the composite fibers conductive, while the conjugated polymer, for example, polydiacetylene derived from a diacetylenic monomer of 10,12-pentacosadiynoic acid, demonstrated a reversible conformation change with a chromatic transition when electric currents were applied. However, the low reversibility and stability of polydiacetylenes limited their practical applications. To this end, side chains were incorporated that had peptide components that formed many hydrogen bonds to further enhance the properties.[113]

Conjugated polymers that change color as a result of a conformation change typically show a limited number of colors, for example, blue and red in the case of polydiacetylene. Multicolored fibers were thus prepared by using conducting polymers as the electrochromic layer with stainless-steel wires as the two electrodes and a polymer gel as the electrolyte (Figure 6b).[114] These electrochromic fibers showed different colors on varying the applied voltages and depending on the electrochromic materials. The color changes were achieved rapidly at low voltages (millisecond level). They could be implanted into fabrics and designed to display a variety of chromatic patterns. However, the use of the stainless steel wire electrode hampered the use of these chromatic fibers in practical applications as it was not as flexible as chemical fibers and was not stretchable. Flexible and stretchable electrochromic fibers have recently been realized by winding aligned CNT sheets onto elastic fibers as electrodes and introducing polyaniline as the electrochromic material.[90] Color changes from green to blue and yellow were observed when charged from 1 to −1 V, and the chromatic transitions could be stably repeated thousands of times. In addition, no apparent damage to the structure or decay of the electrochromatism were observed under bending and stretching.

Electrochromic fibers can also be produced by coating a thermochromic layer onto the electrically conductive core and were compatible with a continuous fabrication by a one-step coaxial melt-spinning process (Figure 6c).[115] They possessed a coaxial three-layer structure consisting of a conductive core layer (polypropylene-CNT), an intermediate layer containing white dye (polypropylene-TiO_2), and a sheath layer containing thermochromic microcapsules. The passage of electric current resulted in a Joule effect from the conductive core layer triggering a color change of the outer thermochromic layer. Electrochromic textiles were also made from electrochromic fibers and showed a color change between green and beige on switching the electric current on and off. As a consequence of the higher electric resistance of the fiber, the required voltages were much higher than the safe voltage for the human body. Therefore, more effort is needed to decrease the fiber resistance to reduce the voltage for chromatism.

4.1.2. Electrochromic Textiles

Besides being woven from electrochromic fibers, electrochromic textiles can be made from real fabrics that are lightweight and comfortable. Spandex is a commercially available and commonly used fabric in our clothes, and it becomes conductive after soaking in a PEDOT:PSS solution.[116] The conductive spandex materials are flexible, deformable, and have a blue color (Figure 7a,b).[116] An electrochromic textile was made by spray-casting an electrochromic precursor onto one side of the conductive spandex and assembling two conductive spandex electrodes face to face so that the modified layers were in contact.[117] The electrochromic textile generated two colors of red and blue as

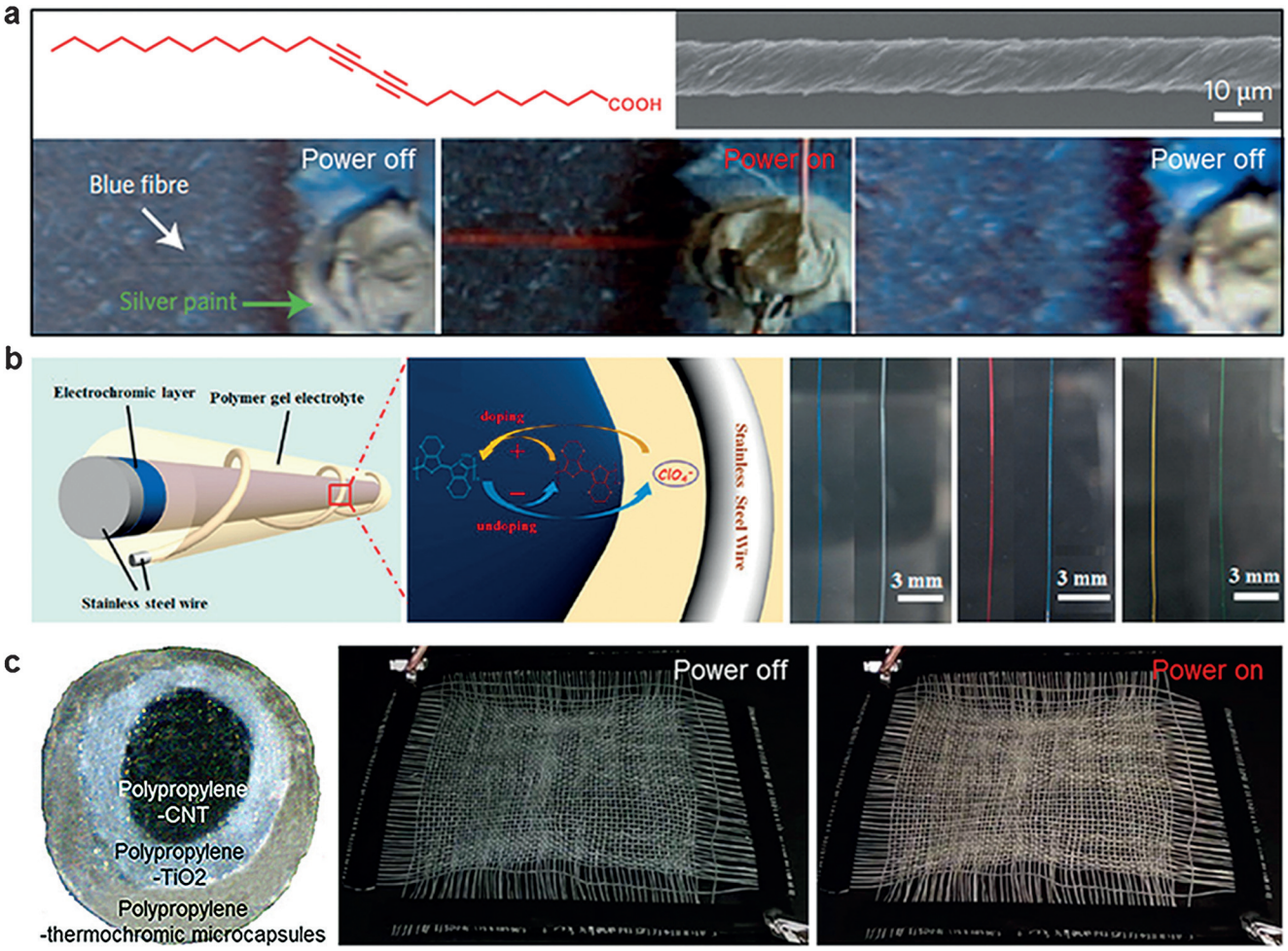

Figure 6. Electrochromic fibers. a) Structure of the diacetylene monomer and the corresponding electrochromatic CNT/polydiacetylene composite fiber upon passage and removal of electric current. b) Structure and photographs of red, green, and blue electrochromic fibers based on the electrochemical effect. c) An electrochromic fiber (diameter of 1 mm) and fabrics based on the electrothermal effect. Reproduced from Refs. [112, 114, 115] with permission. Copyright 2009 Nature; 2014 ACS; 2012 ACS.

a consequence of the different redox states of the electrochromic polymer (Figure 7 c,d). For this structure, a variety of colors could be realized by simply increasing the number of electrochromic polymers; for example, two polymers would generate a reversible four-color combination. The color switch was completed in about 15 s at potentials of −2.0 to +2.0 V.

Similar to electrochromic fibers, electrochromic textiles have also been produced by coating thermochromic inks onto conductive fabrics.[118] For example, conductive PEDOT nanofiber mats were used as electrothermal sources to trigger the color change of thermochromic inks. Although the safety of such electrochromic textiles needs to be further considered because of the requirement of high voltages, the simplicity of this design makes it attractive for the development of flexible materials.

The colors of underlying fabrics will affect the observed colors from the electrochromism through color mixing. A multitude of colored fabrics were coated with PEDOT:PSS as electrodes for electrochromic devices.[119] It was found that brighter and more vibrant colors affected the observed colors through a subtractive mixing effect, but no adverse contrast effects between the two states of the electrochromic materials or devices were observed. This information may be useful for the fabrication of a variety of wearable displays or fashionable patterns with different color combinations by using different conductive fabrics and electrochromic polymers.

4.1.3. Practical Applications

Electrochromic technologies are close to practical applications and are now facing a bright future because of the strong interest for consumer products. For example, Nike has patented the concept of utilizing electrochromic materials to change the color of a pair of sneakers with a smartphone.[120] However, the chromatic performance of the current materials and devices needs to be further improved. More colors and higher stability are required for the polydiacetylene-based electrochromic fibers, while the electric resistance of conductive fibers and fabrics need to be decreased to lower the working voltage and increase the safety of electrothermal chromic textiles. Both systems share a simple structure where

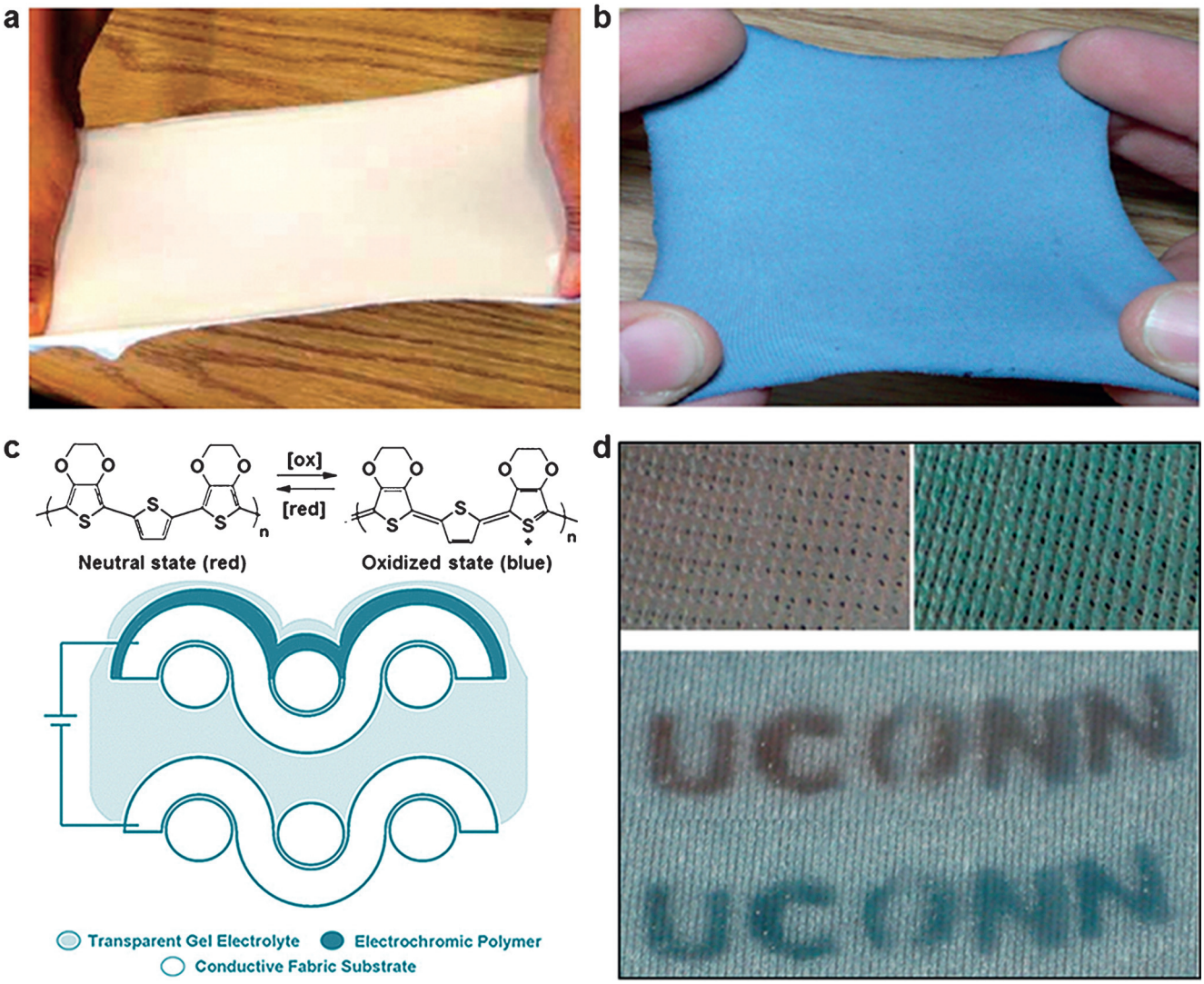

Figure 7. Textile-based electrochromic devices. a,b) Stretchable spandex fabric before and after soaking with PEDOT:PSS. c) Schematic representation of the electrochromic polymer in each redox state, and the cross-section of the all-organic electrochromic spandex fabric device. d) Stretched electrochromic spandex fabric electrode in different states. Reproduced from Refs. [116, 117] with permission. Copyright 2010 ACS; 2010 ACS.

only one conductive electrode is used. For the electrochromic devices using conducting polymers as the active layers, two fiber or fabric electrodes as well as electrolyte are necessary, and two interfaces exist between the electrolyte and the active material and electrode. Those interfaces should be stable enough to tolerate robust operations, particularly for flexible textiles. In addition, the electrode and active materials are sensitive to temperature, moisture, and mechanical stress, thus encapsulation is required for long-term use, which makes the textile airtight and uncomfortable to wear.

Although much effort has been made to synthesize new electrochromic polymers and design new architectures to realize multicolors and wearability, some challenges remain in terms of practical applications.[105,121] For example, the long-term stability of electrochromic materials and devices should be studied further, the contrast/optical brightness remains low, the color variation needs to be broadened, and the light scattering from the rough surface of textiles reduces the optical brightness.

4.2. Electroluminescence

Whereas electrochromic textiles can only work effectively during the daytime or in a place with light, electroluminescent devices can provide bright signs whenever and wherever required by transforming electric energy into light. A typical electroluminescent device is fabricated by sandwiching a phosphor layer between two electrodes, and light is emitted as the molecule in the excited singlet state returns to the ground state when excited by an electric current.[122] The emitted color of an electroluminescent device depends on the phosphors and the dopant materials. Flexible planar organic light emitting diodes (OLED) have been fabricated, which

endured certain mechanical deformations. The key factor for flexible devices is the flexible, transparent, and highly conductive electrodes. Various flexible electrodes have been investigated, including CNT/polymer composite films, modified graphene films, silver nanowire/polymer composite films, and conducting polymer films.[123–129] These efforts represented a major step towards the realization of flexible, stretchable, and wearable electronics.[130] Recently, fiber-shaped electroluminescent devices were also developed for flexible textiles.[131–134]

4.2.1. Electroluminescent Fibers

Based on the fabrication process of planar OLEDs, a fiber-shaped OLED was first fabricated by depositing metal electrodes and active small-molecule layers (tris-(8-hydroxyquinolinato)aluminum) onto the polyimide-coated silica fiber substrate with the assistance of a shadow mask (Figure 8a).[131] It exhibited electrical characteristics and a luminescence efficiency comparable to its planar counterparts. As a consequence of the one-dimensional geometry, the electroluminescent spectrum was independent of the observation angle, which was in contrast to planar OLEDs. This property is important for the use of fiber-shaped OLEDs in textiles because they are observed from different directions. However, the complex fabrication under high vacuum and the low flexibility of the rigid metal wire electrode are not favorable for continuous production and wearable applications. As a result, electroluminescent fibers were developed from liquid metal materials by coelectrospin-

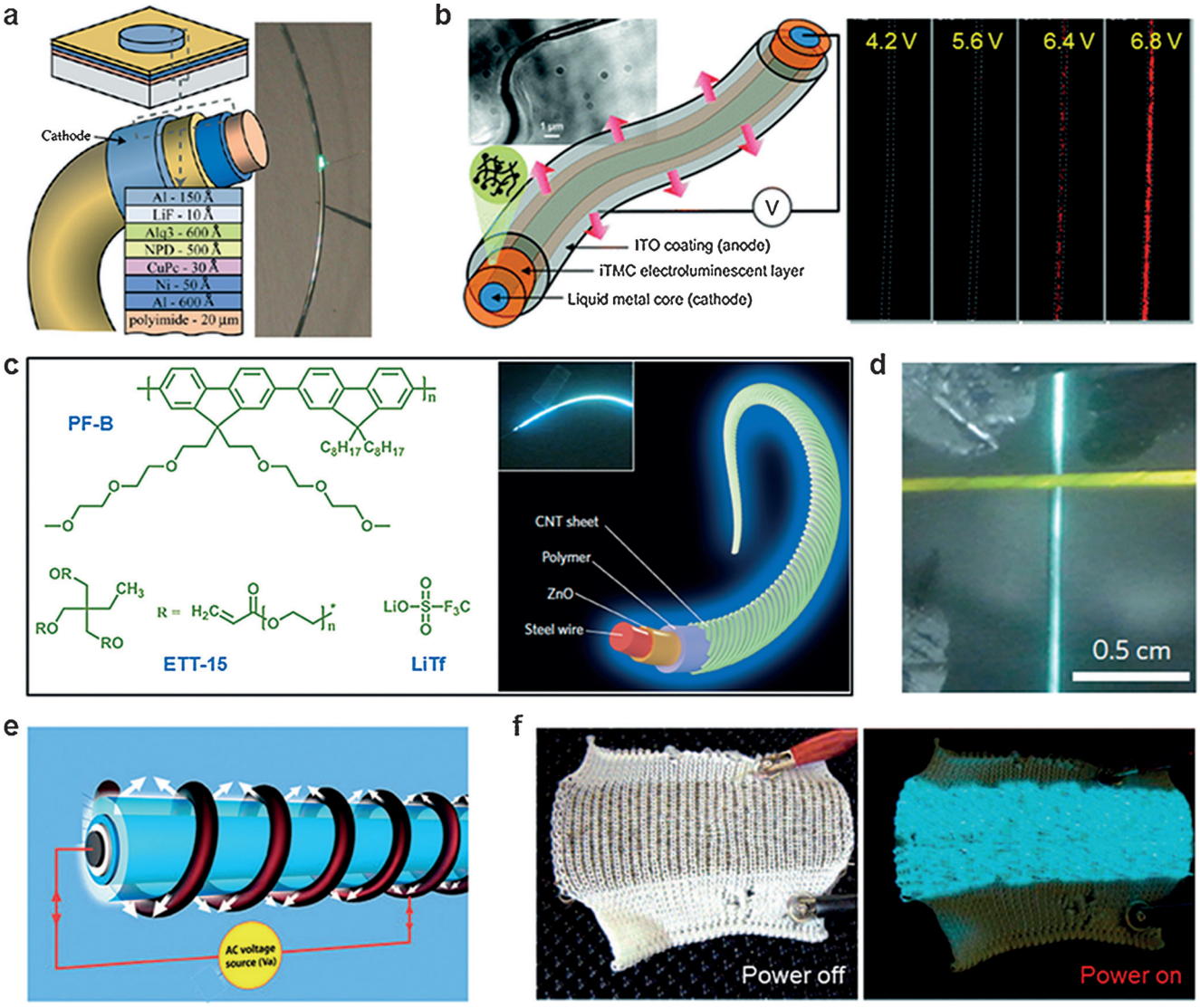

Figure 8. Fiber-shaped electroluminescent devices. a) Fiber-shaped organic light emitting diodes with a similar structure to the planar device (tris(8-hydroxyquinolinato)aluminum as the emission layer). b) Electroluminescent coaxial fibers based on an ionic transition-metal complex with a liquid metal Galinstan electrode. c) Structure of the materials in the emissive layer and the corresponding electroluminescent fiber based on an aligned CNT sheet electrode. d) Knitting of the electroluminescent fiber of (c) into a textile to show the different colors. e) Construction of an electroluminescent fiber based on a silver-coated polyester fiber. f) Polyester fabric containing electroluminescent fibers in non-excited and excited states. Reproduced from Refs. [131–134] with permission. Copyright 2007 Wiley-VCH; 2012 ACS; 2015 Nature; 2012 SAGE.

ning.[132] They consisted of three coaxial layers, namely, liquid metal Galinstan as the cathode core, an active ionic transition-metal complex layer in the middle, and an indium-tin oxide thin film as the anode at the outer layer (Figure 8b). They exhibited increasing luminance intensities as the voltages increased, and the electroluminance could be detected by a camera and seen by the naked eye. For these electroluminescent fibers, it was necessary to seal them to avoid leakage of the liquid metal materials, and the connection of the liquid core requires a thin tip, which was inconvenient for application. To this end, flexible and conductive solid materials such as conducting polymers, CNTs, and graphene may be proposed to replace the liquid metal core to prevent the above problems, but more studies are required to verify the possibility of this strategy.

Recently, a novel electroluminescent fiber was also designed with a coaxial structure, including a modified metal wire cathode and a conducting aligned CNT sheet anode with the electroluminescent polymer composite layer sandwiched between them (Figure 8c).[133] Electroluminescent polymers could be easily coated by solution processes. Aligned CNT sheets could be uniformly wrapped onto the metal wire to function as an anode because of its high transparency (>87% at 550 nm), conductivity (10^2–10^3 S cm^{-1}), flexibility, and stability. The resulting electroluminescent fibers exhibited tunable colors on varying the voltages (5.6–13 V) and electroluminescent layers (blue, yellow, and their combination) with a high luminance of 609 cd m^{-2}. In addition, these electroluminescent fibers were flexible and the brightness could be maintained at over 90% after bending 100 times. Therefore, they could be knitted into textiles to show different colors and patterns (Figure 8d). Although the driving voltage was slightly higher than the conventional OLED because of the relatively low conductivity of the CNT sheet anode, the fabrication process allows for large-scale production.

Metal wires have been typically used for the electroluminescent fibers because of their high electrical conductivities and low costs. However, they are not elastic and have low flexibility, so the replacement of elastic conductive fibers will be more useful for wearable devices. A continuous electroluminescent fiber was constructed with the silver-coated polyester fiber as the base electrode, followed by coating with a dielectric insulation layer, electroluminescent layer, and dielectric transparent layer and then helically winding a Cu wire electrode (Figure 8e).[134] It showed tunable luminances on varying the frequencies of the applied voltages (Figure 8f). However, it required a much higher threshold voltage of 90 V than the other systems. Furthermore, the luminance was not uniform, possibly because of the presence of the insulating layer. It may be used in fields with high power outputs, such as in automobiles, after optimization.

4.2.2. Electroluminescent Textiles

Electroluminescent textiles woven from fibers were discussed above, and they were also made onto soft fabrics. The fabric electrodes must be simultaneously transparent, conductive, and flexible. In a typical fabrication, PEDOT:PSS was printed on a monofilament mesh fabric as an electrode; an electroluminescent textile was produced by sandwiching phosphor and dielectric layers between the front fabric electrode and a rear Al electrode (Figure 9a,b).[135] The highest luminance intensity reached 44.0 cd m^{-2} at 400 V and 400 Hz. To further enhance the luminance performance, other highly conductive materials such as CNTs were further introduced to the conductive layer on the fabrics (Figure 9c).[136]

The previous fabrics typically exhibited low luminous efficiencies and needed high operating voltages. Recently, OLEDs were designed on commercial polyester fabrics (Figure 9d,e).[137] They showed a low driving voltage of 2.5 V, with a luminance of 3.04 cd m^{-2} and a current efficiency of around 8 cd A^{-1}. They were lightweight and flexible, and no significant changes in the electrical or optical characteristics were observed after bending (radius of 5 mm) 1000 times. However, the tensile strain was low and they were unable to tolerate stretching and twisting. In addition, the emitted colors were shifted depending on the angle of observation. To summarize, electroluminescent textiles have advantages and disadvantages and should be used according to the required application.

4.2.3. Practical Applications

To more effectively take advantage (deformability, breathability, and comfort) of electroluminescent textiles, it is better to realize the electroluminescence at the fiber level.[138] The electroluminescent fibers can then be integrated into textiles by weaving, knitting, embroidery, lamination, or stitching. The integration of LEDs mounted on lightweight flexible substrates into clothes can nowadays be achieved on a commercial scale. Lumalive from Philips represents an effort to weave fibers with LEDs into textiles. Philips also developed a baby blanket which can provide infants with light therapy.[138] However, some difficulties remain for the large-scale application of electroluminescent fibers and textiles. For example, the low luminous efficiency and high operating voltages are critical barriers to wearable electronics, and the stability needs to be further increased for long-term use.

4.3. Electromechanical Actuation

Electrically driving actuators have been widely explored for mechanical applications such as robots. They are usually composed of active materials that can change shapes and dimensions upon the use of electricity.[138] The most promising active materials for smart textiles are electroactive polymers which have the advantage of being lightweight, soft, and flexible. The electroactive polymers can also be easily processed with inorganic materials. However, electrically driven fiber and fabric actuators are rare. The available examples are mainly based on CNT fibers or their composites.

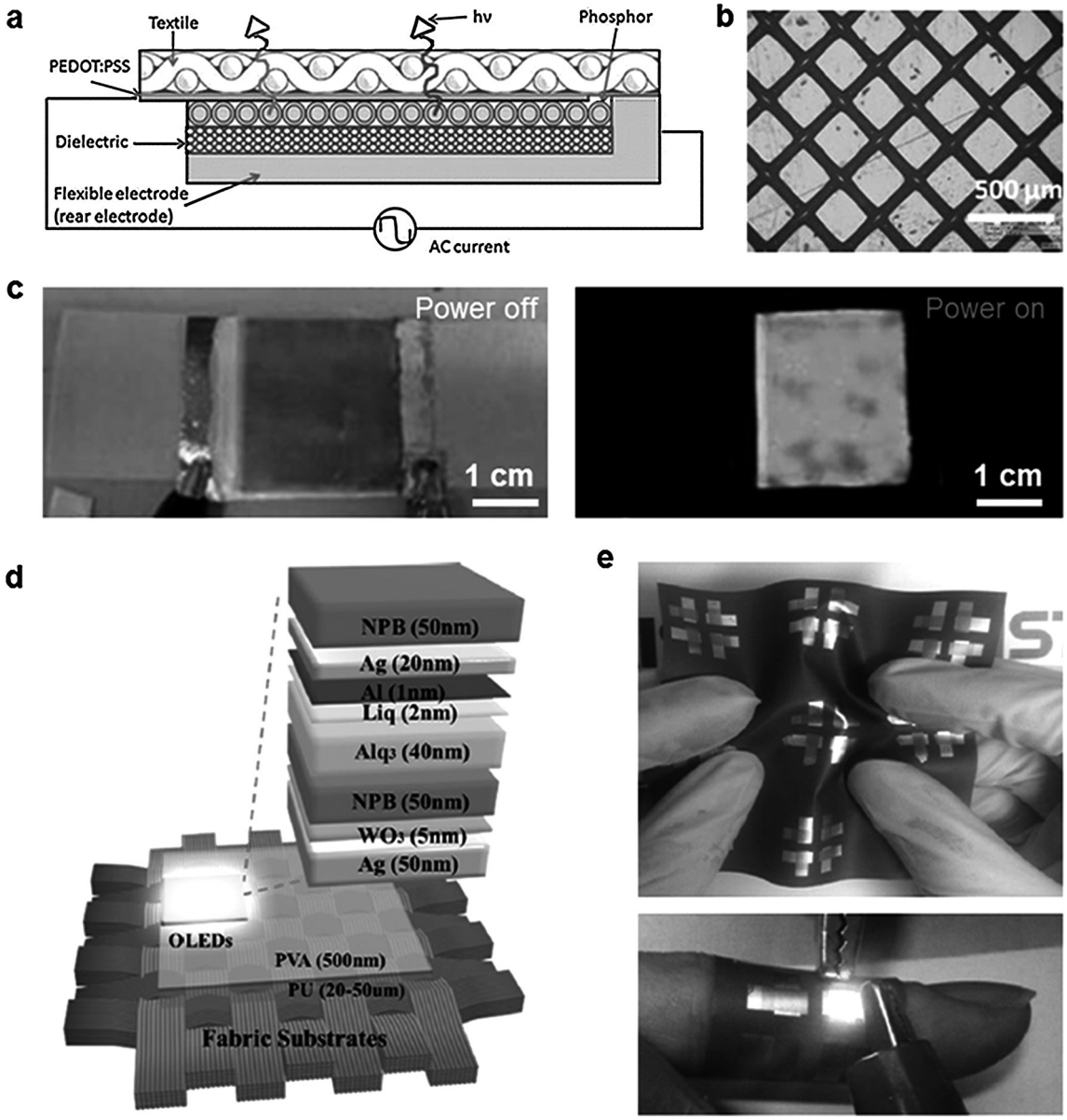

Figure 9. Textile-based electroluminescent devices. a) Schematic illustration of a flexible electroluminescent fabric. b) Poly(ethylene terephthalate) mesh with printed PEDOT:PSS. c) Electroluminescent device based on poly(ethylene terephthalate)/CNT/PEDOT/nylon before and after applying a voltage. d) Soft fabric organic light emitting diode with an emission layer of tris(8-hydroxyquinolinato)aluminum. e) Photographs of the soft organic light emitting diode fabric under folding (top) and light (bottom). Reproduced from Refs. [135–137] with permission. Copyright 2011 Wiley-VCH; 2012 RSC; 2013 Elsevier.

4.3.1. Electromechanical Carbon Nanotube Fibers

To the best of our knowledge, the first CNT actuators were reported to actuate with contraction and expansion as a response to charge injection and extraction.[139] Many subsequent studies aimed to improve the actuation performance by changing the electrolyte and assembly of the CNTs. In general, aligned CNTs are favorable for electromechanical actuators with large and rapid actuation responses. It was found that the aligned CNT fibers generated stresses one order of magnitude higher than the entangled CNTs.[140] Various aligned CNT assemblies including arrays and sheets also showed electromechanical actuation.[141–144] However, these actuators typically resulted from charge ingress and outflow and were usually investigated in liquid or gel electrolytes, which is difficult for portable and wearable applications.

Recently, aligned CNT fibers were found to act as highly efficient actuators in air through a different mechanism, namely, the electromagnetic effect.[145–148] Electromechanical actuations were first realized in a bare CNT fiber with highly reversible contraction, rotation, and self-twisting.[145] The actuation could be performed by directly passing a low direct electric current in air without any electrolyte. The contraction strain and rotation angle exceeded 2% and 360°, respectively. It was proposed that Ampere's Law among

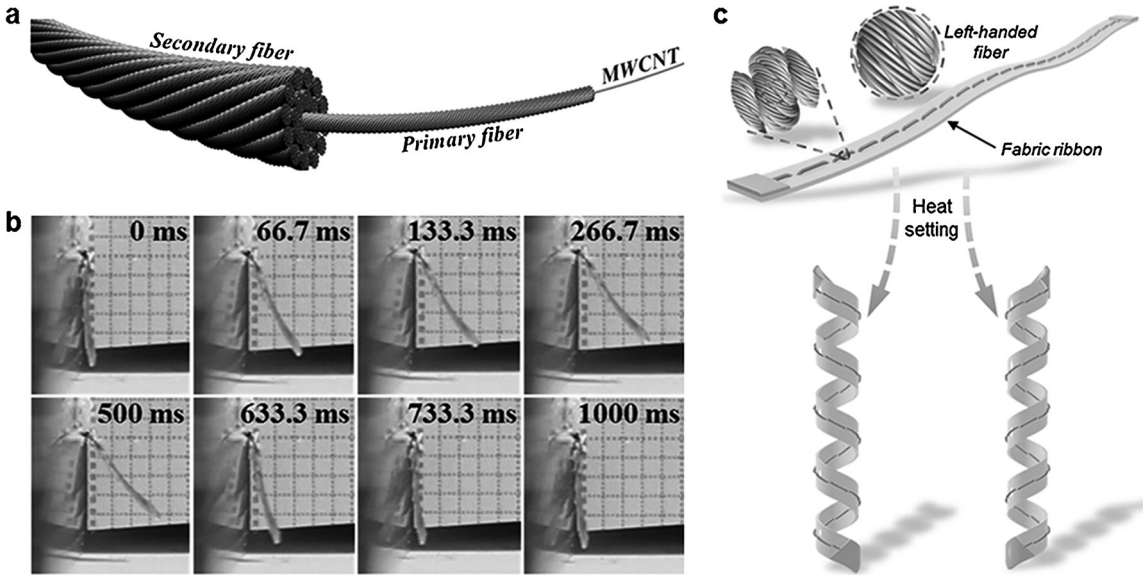

Figure 10. Electrically deformable fibers. a) A secondary CNT fiber helically assembled from primary CNT fibers. b) Flapping motion of an artificial wing based on secondary CNT fibers. c) Fabric ribbon actuator by weaving CNT fibers (with a coiled structure) into a Kapton film. Reproduced from Refs. [146, 149] with permission. Copyright 2015 Wiley-VCH; 2015 Wiley-VCH.

helically aligned CNTs contributed to the longitudinal contraction and torsional rotation.[145] The microstructure of the CNT fibers played an important role in enhancing the performances and behaviors of the actuators.[146] A secondary CNT fiber was prepared by twisting a bundle of primary CNT fibers (Figure 10a). It produced sophisticated and controlled motions similar to a spring, a wing, or a tail upon application of electric current (Figure 10b). Moreover, the generated stress was magnified from the primary to the secondary fibers under similar electrical power densities as a result of the hierarchical microstructures within the secondary fiber. It was further found that both contractive strain and rotation outputs triggered by electricity could be enhanced by forming coiled structures through an over-twisting process.[149] The resulting fibers could be readily woven into polymer films to prepare fabric ribbon actuators with programmable motions including bending, rotation, contraction, and elongation (Figure 10c). Other mechanical responses including a change in modulus, collective electromagnetic forces, and densification (contraction) were also found when electric currents were passed through the CNT fibers.[147]

Electrothermal heating can also trigger the actuation of CNT fibers by a structural transformation of infiltrated guest materials. A coiled CNT/paraffin wax composite fiber exhibited a tensile actuation of 1200 cycles per minute and a 3% stroke over more than 1.4 million cycles.[150] The performances could be enhanced by decreasing the coil diameter and increasing the voltage. However, the high applied electrical power reduced the cycle life by causing excessive heating and evaporation of the paraffin.[147] Similar to the multiwalled CNT fibers twisted from aligned CNT sheets, helical single-walled CNT fibers could be twisted from spider-web-like thin films of single-walled CNTs to form uniform, closely arranged loops along the fiber length.[151] Wax was then incorporated to form composite fibers that produced a strain of 90% or a stress higher than 15 MPa under a voltage of not higher than 2 V. These actuations were attributed to both electromagnetic attraction of the CNTs as well as volume expansion of the wax. For practical applications of CNT-based fibers in smart textiles, hierarchical structures and composites can be designed to meet the requirements of different actuations.

4.3.2. Electrothermally Driven Polymer Composite Actuators

Electrothermally active polymer composites can undergo expansion/contraction and bending upon the application of electricity. These polymer actuators are stable in air without the need for electrolytes. Shape-memory polymers have been made into textiles in the form of fibers, films, and foams, and usually activated by heating. Electricity can also simulate the shape-memory effect of polymers by electroheating above the switching temperature after incorporating conductive fillers such as carbon nanomaterials.[152,153] These fillers provide an electrically conductive network and a Joule heat resource as well as enhancing the mechanical properties of the polymers. Electroactive shape-memory fibers were developed by incorporating CNTs into shape-memory polymers.[154] These composite fibers were first stretched at high temperatures and cooled to room temperature under external stress. Upon application of a voltage of 210 V, these composite fibers began to shrink and finally recover to their original length. However, the shape recovery ratio, fixing ratio, and stress need to be further enhanced, possibly by increasing the dispersion and alignment of the CNTs to satisfy the requirements for textile applications. The voltage used also needs to be decreased for safety.

5. Multifunctional Electronic Textiles

Electronic textiles with a single function can not meet the requirements for electronics. Increasing attention has thus been paid to realize the functional integration among the generation, storage, and utilization of electricity and the introduction of other functionalities into electronic textiles. The mainstream directions of such an integration are summarized below.

5.1. Integration of Generation, Storage, and Utilization of Electricity

5.1.1. Generation and Storage of Electricity

To realize self-powering electronics, it is necessary to generate and store electricity in one textile. The main efforts are currently focused on integrating DSSCs and supercapacitors as their materials, structure, and fabrication methods are compatible. In a simple model, a modified Ti wire and an aligned CNT fiber, one part of which was coated with a photoactive material for photoelectric conversion while the other part had electrochemically active materials deposited on it for energy storage, were twisted into an integrated fiber for the generation and storage of electricity. It exhibited a power conversion efficiency of 2.2% and energy-storage efficiency of 68.4%, which produced an overall efficiency of 1.5%.[155] To further increase the performance of the multifunctional fiber, a coaxial structure was developed by winding aligned CNT sheets to replace the CNT fiber. The photoelectric conversion and energy-storage efficiencies reached 2.73% and 75.7%, respectively; the overall efficiency was then calculated to be 2.06%.[156] The use of liquid electrolytes for the photoelectric conversion is incompatible with continuous fabrication and long-term application. Therefore, polymer solar cells instead of DSSCs were integrated with the supercapacitor, and an all-solid-state fiber-shaped integrated device was produced with improved flexibility and stability. However, the power conversion efficiency of the polymer solar cell was lower than the DSSC, and so the overall electricity generation and storage efficiency of the all-solid-state fiber were greatly decreased. The multifunctional fiber-shaped devices could be woven into commercial textiles.[157]

As both solar cells and supercapacitors can be incorporated into stretchable fibers and textiles, the integrated multifunctional devices can also be stretchable. For example, a stretchable fiber-shaped supercapacitor was first fabricated, followed by insertion into a spring-like modified Ti wire photoanode and winding with an aligned CNT sheet counter electrode for photoelectric conversion.[158] The overall energy conversion and storage efficiency reached 1.83%, a value that was similar to that of the nonstretchable counterpart.

The above-mentioned fiber-shaped integrated device contains two parts for different functionalities, and they usually share one electrode or connect two parts by additional conductive wires. For simplicity, an all-in-one device was realized by simultaneously introducing photoactive and electrochemically active materials between two twisted fiber electrodes.[159] It exhibited a power conversion efficiency of 6.58% and a specific capacitance of 85.03 $mF\,cm^{-1}$, and the two functionalities could be alternately realized without sacrificing either performance.

Piezo- and triboelectric nanogenerators could also be integrated with a supercapacitor and lithium ion battery based on modified carbon cloth electrodes, respectively.[160,161] The electric energy was generated from mechanical energy and stored in the form of electrochemical energy. In addition, multiple electric generators can be integrated simultaneously with electrochemical storage devices to store electric energy harvested from different sources in the environment. For example, electric energy can be generated from solar and mechanical energy and stored in the supercapacitor by integrating a DSSC, PENG, and supercapacitor in one fiber. A polymer fiber coated with Au and ZnO nanowire arrays was used as the common electrode, and copper meshes covered with graphene was wound on the fiber to act as another electrode. The PENG part was obtained directly, while the DSSC and supercapacitor parts were filled with liquid and gel electrolytes, respectively. However, the solar energy conversion efficiency was extremely low (0.02%) because of the low transparency of the Cu mesh, and the specific capacitance of 0.4 $mF\,cm^{-2}$ was slightly lower than other fiber-shaped supercapacitors. Although the overall electricity generation and storage efficiency was relatively low, it provided a promising model for the development of multifunctional devices.

5.1.2. Electric Storage and Utilization

As previously mentioned, electric energy can be stored electrochemically in supercapacitors, while electrochromism can be realized through the electrochemical redox reactions of conducting polymers. Thus, the integration of electric storage and utilization is promising for wearable textiles with self-powered chromatic transitions or self-monitoring of the working state. To this end, an electrochromic fiber-shaped supercapacitor was developed by electrodepositing polyaniline onto aligned CNT sheets wound on elastic fibers.[90] It exhibited a specific capacitance of 255.5 $F\,g^{-1}$, an energy density of 12.75 $W\,h^{-1}\,kg^{-1}$, and a power density of 1494 $W\,kg^{-1}$. In addition, it showed different colors including blue, green, and light yellow during the charge/discharge processes. The chromatic transitions were rapid and reversible, which could be used to indicate the working states of supercapacitors effectively. The capacitance and electrochromism were both stable under bending and stretching hundreds of times. These electrochromic fiber-shaped supercapacitors could be further woven into fabrics to display designed patterns.

5.2. Integration with Sensing Functionality

In addition to the generation, storage, and utilization of electricity, it is necessary to endow the electronic textiles with other functionalities. Of these, sensing environmental change has been mostly explored in electronic textiles because of promising applications in many fields such as intelligent

control, personal protection, healthcare, and early warning.[138,162–164] Here, typical fiber and textile sensors are first summarized according to their different stimulations including mechanical stimuli, temperature, chemical substances, and humidity.

5.2.1. Strain and Pressure Sensors

Among the electronic sensors, those responding to mechanical stimuli such as strain and pressure have been mostly explored.[165] Generally, electronic fiber/textile sensors responding to strain and stress can be divided into three types according to the different sensing mechanisms, namely, resistive, capacitive, and self-powering. In the case of resistive sensors, a change in the electrical resistance occurs when the geometry of the fiber/textile deforms upon the application of strain and stress. The capacitive sensor is typically composed of a dielectric layer sandwiched between two conductive layers.[166] The capacitance changes with the variation of the thickness of the dielectric layer caused by the mechanical stimulus. Self-powering sensors are typically made from piezoelectric materials and can generate electronic signals upon mechanical stimuli without external power sources.

Resistive Sensors

Resistive fiber sensors transform a change in the resistance into a measurement of the strain and have been extensively investigated because of their simple structure. The change in the resistance can be derived from several factors including changes in the deformation of the fiber/textile, the contact resistance between the conductive components, and the resistivity of the composite fiber caused by the separation of conductive additives. Both electrical conductivity and stretchability are critical for electronic strain/pressure sensors.

Typically, a variety of conductive materials including conducting polymers, carbon materials, and metallic nanowires are used as the conductive layers, while commercial polymer fibers such as polyamide 6, Lycra, polyolefin, and polyurethane serve as the elastic substrates. Polypyrrole and PEDOT:PSS are the two mostly explored conducting polymers because of their acceptable electrical conductivities and piezoresistive properties. They can be coated onto commercial polymer fibers to form a conductive layer through various techniques such as solution dipping, in situ polymerization, and chemical vapor deposition.[167–169] However, the conductive layers are unstable during stretching because of the smooth surfaces of the polymer fibers.[167,168] To solve this problem, structural defects or chemical groups are produced on the surface of the fiber substrate to enhance the interfacial adhesion between the substrate and conductive layer.[169] The fiber sensors are still not very stretchable (e.g. a low strain of 1.5%) and exhibit an unstable sensing performance as a result of the mismatch between the conductive and substrate polymer fibers.

The stretching mismatch between the conductive layer and polymer fiber substrate can be efficiently avoided through compositing processes instead of coating methods. A composite fiber of polyurethane and PEDOT:PSS was capable of monitoring a wide strain range up to 260%, which is hundreds of times higher than that of the fiber coated with conductive layers.[170] Metallic nanowires with high electrical conductivities could also be introduced into the polymer matrices to show better performances. For example, a styrene-butadiene-styrene fiber embedded with silver nanowires could be readily obtained by a wet-spinning process, followed by adsorption and reduction of the Ag precursor (Figure 11 a,b).[171] The resulting composite fiber exhibited a high electrical conductivity of 2450 $S\,cm^{-1}$ and a breaking strain of 900%. The fibers could be woven into gloves for detecting gestures and human motions. Other conductive nanowires or nanoparticles could also be introduced into the stretchable fiber substrates to achieve sensing functions.[172,173]

Although the composite fiber sensors are promising in a variety of applications, the compositing processes are rather complex. To this end, some intrinsically conductive materials without guest materials have been developed to directly serve as strain and pressure sensors. A wet-spun PEDOT:PSS fiber, after hot drawing and doping/removal of ethylene glycol, exhibited a high conductivity of 2800 $S\,cm^{-1}$, which is much higher than that of the composite one.[174] The fiber could be used to sense cyclic stretching with a strain up to 20%. However, the polymer-based fiber sensors suffered from low stability during sensing. CNTs have been extensively investigated for several decades because of their combined high mechanical and electrical properties.[175] Among them, aligned CNT fibers with strengths of about 10^3 MPa and conductivities of about 10^3 $S\,cm^{-1}$ have been studied for strain sensors.[176,177] A spring-like CNT fiber was prepared that exhibited high breaking strains up to 285%,[178] and it demonstrated a reversible and linear change of resistance in response to strain (Figure 11 c).[179,180] Similarly, reduced graphene oxide fibers or ribbons were also explored for use as strain sensors.[181] However, the scale-up fabrication of high-quality CNTs and reduced graphene oxide fibers remains challenging. At present, fiber sensors prepared by a compositing method are competitive candidates for smart textiles on a large scale.

Three strategies are used to develop electronic textiles to sense external strain and stress: 1) fiber sensors are woven into electronic fabrics;[182,183] 2) fiber sensors are integrated into commercially available textiles such as clothes and gloves;[184–187] 3) functional materials are deposited onto commercial textiles.[188–191] Furthermore, the electrospinning technique represents a novel one-step strategy to fabricate electronic textile sensors.[192–194] Conducting polymers, for example, PEDOT:PSS and polyaniline, have been used to make electrospun nonwoven mats with a strain-sensing property.[195,196] In particular, the woven mats exhibited a higher sensitivity as a consequence of the higher specific surface area of the building nanofibers.

Capacitive Sensors

For capacitive sensors, the mechanical stimulus is transformed into electric signals based on the principle of a capacitor.[165,166] Typically, a planar capacitive sensor is

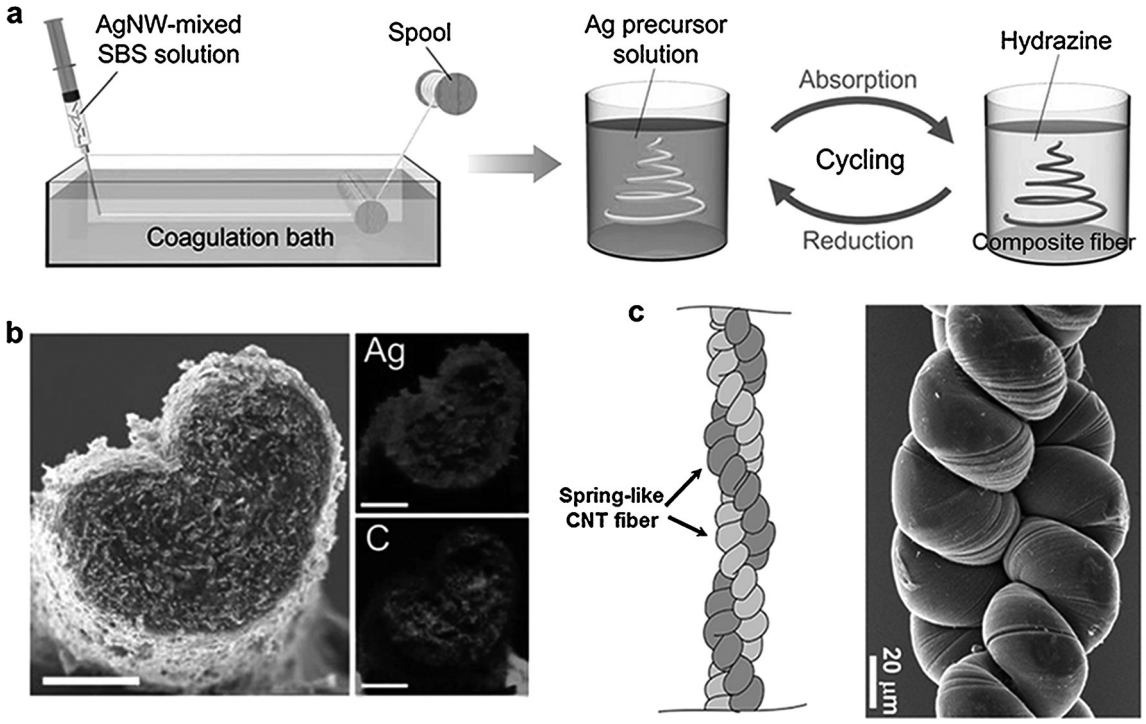

Figure 11. Resistive sensors in response to strain and pressure. a) Schematic illustration of the fabrication of a fiber sensor composed of Ag nanowires and styrene-butadiene-styrene. b) SEM image of the composite fiber with a weight percentage of Ag nanowires at 0.56%, and energy-dispersive spectrometry mapping images of Ag and C embedded within the fiber. Scale bar: 100 μm. c) Optical images of the composite fiber before and after stretching by 900%. d) Illustration and SEM image of the over-twisted double-helix CNT fibers. Reproduced from Refs. [171, 179] with permission. Copyright 2015 Wiley-VCH; 2013 ACS.

composed of a dielectric layer sandwiched between two electrically conductive layers. The capacitance (C) of a parallel plate capacitor was obtained according to the equation of $C = \varepsilon_0\varepsilon_r A/d$, where ε_0 and ε_r are the free space permittivity and relative permittivity, respectively, A is the plate area, and d is the distance between the two parallel plates. The specific capacitance of the sensor varies as a result of changes in the variables A, d, and ε_r caused by mechanical stimuli. The capacitive sensors have many advantages for sensing, such as high sensitivity and low energy consumption.[165]

Similar to the planar capacitive sensor, a fiber-shaped capacitive sensor is also composed of two components, namely, electrodes and an intermediate dielectric elastomer. Insulating fibers or fabrics could be endowed with electrical conductivity after incorporating them with electrically conductive materials such as conducting polymers, metal nanowires, and CNTs.[165,197,198] Elastic polymers such as polydimethylsiloxane and polyurethane can serve as the dielectric elastomer.[166,199] Recently, a novel capacitive strain fiber sensor with a multicore-shell structure was fabricated through a coextruding approach (Figure 12a,b).[200] The fiber was composed of alternating layers of conductive ink and dielectric elastomer, and could accurately detect both static and dynamic strains as well as shearing stimuli without notable hysteresis. The elastic fiber sensor could be readily woven into textiles to monitor human motion and showed great potential for wearable electronics. Complicated equipment and preparation methods are required for fiber sensors with a four-layered coaxial configuration, which are not favorable for large-scale production. Alternatively, a novel capacitive sensor was developed from two stacked conductive fibers coated with polydimethylsiloxane (Figure 12c).[201] In comparison with the all-in-one fiber sensors, the capacitance of this sensor was generated by incremental contact between the two perpendicularly crossed polydimethylsiloxane-coated fibers under mechanical stimuli. The empty space near the contacting region endowed the sensor with an efficient and rapid decrease in the distance between the encapsulated conductive fibers (Figure 12d). Therefore, the capacitive sensor exhibited high sensitivity and stability, and could be woven into clothes to wirelessly control machines through gestures (Figure 12e).

Many methods have been explored to fabricate capacitive textile sensors. Among them, weaving the capacitive fiber-shaped sensors into the commercial textile is the simplest.[198,200,201] However, it is difficult to continuously fabricate fiber sensors and then weave them into commercial textiles. In addition, the fiber sensors are currently too thick and mismatched with traditional textile threads. Furthermore, the outer functional layer is vulnerable to damage during weaving. Alternatively, some attempts have been made to fabricate capacitive textile sensors from commercially available textiles with a sandwiched configuration.[202] The textile electrodes could be endowed with conductivity through the introduction of conductive materials.[162,203] Similar to the panel capacitors, the two textile electrodes were separated by

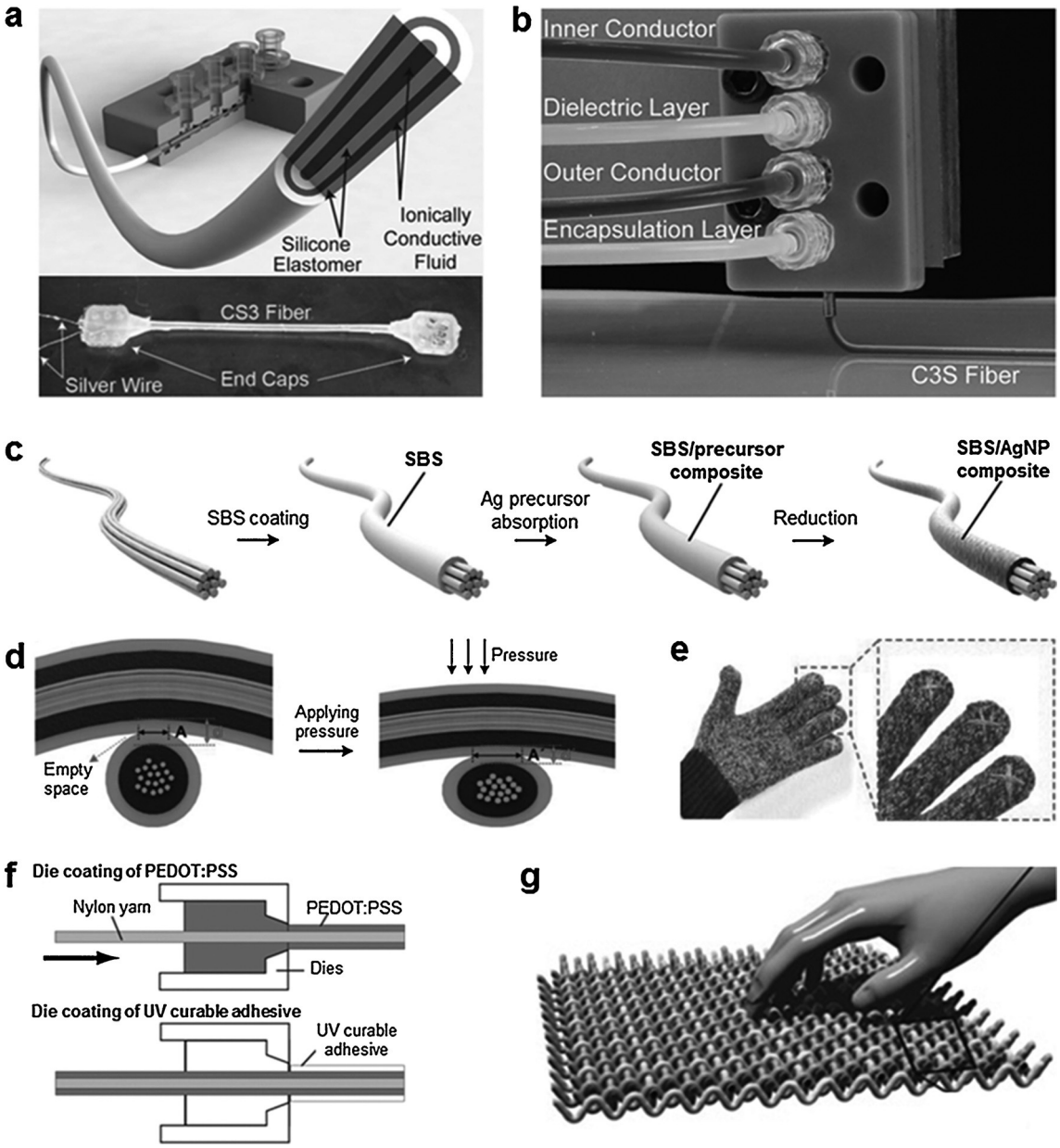

Figure 12. Capacitive textile sensors. a,b) Schematic illustration and photograph of the capacitive fiber sensor with a multicore-shell structure. c,d) Schematic illustrations of the fabrication and sensing mechanism of a capacitive fiber sensor composed of a Kevlar fiber core, a conductive layer of styrene-butadiene-styrene/Ag nanoparticle composite, and a dielectric layer of polydimethylsiloxane. e) Photographs of a smart cotton glove woven with the pressure fiber. f) Schematic illustration of the preparation of capacitive fiber sensors with a multicore-shell structure. g) Schematic illustration of a capacitive textile sensor woven from multicore-shell fibers. Reproduced from Refs. [199, 202, 205] with permission. Copyright 2015 Wiley-VCH; 2012 Elsevier; 2014 Elsevier.

an insulating textile to form a textile sensor.[204] The resulting textile sensor could be fabricated on a large scale and showed high accuracy.

In contrast to the layered structure, textiles could also be obtained on a large scale for pressure sensing by weaving fibers coated with conductive and dielectric layers (Figure 12 f,g).[199] The capacitors were formed at the crossing points between the weft and warp fibers and varied according with the change in the distance between them under pressure (Figure 12 g). The fabric capacitive sensors were used as wearable keyboards by weaving the coated fibers with an array configuration. It was also found that the capacitor could be formed between the fibers and human fingers upon touching, because the human body is electrically conductive and could serve as an electrode.[205] They could be used as lightweight and flexible keyboards for wearable applications.

5.2.2. *Temperature Sensors*

Sensing environmental and human body temperature is another important functionality for smart wearable sensors. Several metallic wires such as Cu, W, Ni, and Pt demonstrate

intrinsically resistive sensitivity to temperature.[206] Among them, the platinum wires exhibited a high precision of 0.003% for a temperature change of 0.03 °C, and could be integrated into elastic membranes for clinical use.[207] In general, the metallic temperature-sensitive wires could be integrated into commercially available fabrics by various weaving techniques.[208] The resulting smart textile exhibited linear temperature-resistance relationships. Although the smart textiles with embedded temperature-sensitive metallic wires are structurally simple and can be readily scaled up, they unfortunately suffered from various disadvantages including a heavy weight and limited stretchability.

Polymer composites with conductive or temperature-sensitive additives demonstrated high flexibility and large changes in resistance in response to temperature variations. Many kinds of additives such as CNTs, carbon black, carbon fibers, and metallic particles can be incorporated into polymer fibers by using wet-spinning, melt-spinning, and coating methods.[209–212] An increase/decrease in the experimental temperature resulted in the composite fiber sensors exhibiting resistance variations because the thermal expansion/contraction of the polymer matrix modified the conductive networks in the fiber. It was also demonstrated that the composite fiber composed of multiple polymers and/or additives, for example, by mixing matrixes of polyethylene/poly(ethylene oxide) with Ni particles, could efficiently enhance the sensing reproducibility within a tunable temperature range.[213] The newly developed fibers based on carbon nanomaterials are more promising as textile sensors to detect temperature changes. An over-twisted double-helix CNT fiber with a high stretchability of more than 200% was reported to exhibit a linear resistance-temperature dependence within the temperature range of 40 to 120 °C.[179]

Self-powering wearable temperature sensors were fabricated from thermoelectric materials including inorganic and conducting polymers.[29,214,215] A fabric-based thermoelectric sensor was demonstrated by incorporating Bi_2Te_3 and Sb_2Te_3 through a screen printing technique.[29] The resulting sensor was thin and flexible, and thus could be utilized to monitor body temperature with high stability. However, the inorganic fiber or textile sensors still suffer from the disadvantages of stiffness and small stretching strain. Recently, it was reported that reduced graphene oxide foam also possessed a temperature sensitivity based on the thermoelectric effects in the graphene.[216] The conductive graphene oxide foams could sense heat/cold and measure the dimensions of the heated/cooled area. They are lightweight, flexible, and stretchable, thus could be integrated into commercial cloths and fabrics.

5.2.3. *Sensors for Chemicals*

Rapid and accurate determination of chemical gas is of practical importance in the workplace and as a safety measure in an unknown environment. The present chemical sensors are mainly made of semiconductor metal oxides, conducting polymers, and carbon materials.[217–219] These materials can be fabricated into fiber-shaped chemical sensors for the detection of toxic vapors, including nitric oxide and ammonia. These fibers include porous carbon fibers with TiO_2 and CNTs additives,[220] pitch-based carbon fibers,[221] polyaniline-coated optical fibers,[222] and CNT-coated poly(ethylene imine)/cotton yarn.[223] Their performances are presented in Table 1. The fiber-shaped sensors were flexible and could be knotted and woven into commercial textiles. However, fiber sensors first need to be produced on a large scale to realize textile-shaped sensors.

A simpler way to fabricate chemical fabric sensors on a large scale is to coat the sensing material on the fabric. Various conducting polymers such as polyaniline and polypyrrole have been coated on the surface of poly(ethylene

Table 1: Summary of fiber- and textile-shaped chemical sensors.

Type	Material[a]	Detected gas	Detection limit	Ref.
ceramic	TiO_2/porous carbon fibers	NO	5 ppm	[220]
	V_2O_5	NH_3	0.85 ppm	[257]
CNT	SWCNT/cotton yarn/PEI	NH_3	n.a.	[223]
	F-SWCNT/(PVC, cumene-PSMA, PSE and PVP)	body odors	50 ppm	[258]
	CNT/nylon-6	various polar and nonpolar gases	n.a.	[259]
	CNT/SnO_2	CO	47 ppm	[260]
polymer	polypyrrole/PET; polyaniline/PET	DMMP, NH_3, NO_2	21 ppm	[224]
	polyaniline/optical fiber	NH_3	50 ppm	[222]
	poly(vinyl butyral)	acetone	50 ppm	[261]
	polypyrrole/PET	NH_3 and HCl	n.a.	[225]
	poly(diphenylamine)/PMMA	NH_3	1 ppm	[262]
	PEDOT/poly(vinyl alcohol)	NH_3	5 ppm	[228]
	polyaniline/poly(ε-caprolactone)	NH_3, NO_2	2.5 ppm	[229]
	polypyrrole/poly (vinyl sulfonic acid sodium salt)	ethanol, ozone	0.01 ppm	[227]
	PMMA/polyniline	$(C_2H_5)_3N$	20 ppm	[230]
	poly(vinyl alcohol)/polyaniline	amines	100 ppm	[263]
	polyaniline/nylon 6	NH_3, CO, C_3H_8	1000 ppm	[226]

[a] PEI: poly(ethylene imine), PET: poly(ethylene terephthalate), F-SWCNT: functionalized single-walled carbon nanotube, PVC: poly(vinyl chloride), cumene-PSMA: cumene-terminated poly(styrene-*co*-maleic anhydride), PSE: poly(styrene-*co*-maleic acid) partial isobutyl/methyl mixed ester, PVP: poly(vinyl pyrrolidone), PMMA: poly(methyl methacrylate), PVS: poly(vinylsulfonic acid methyl ester), DMMP: dimethylmethylphosphonate.

terephthalate) and nylon textiles to develop chemical sensors.[224] However, chemical sensors made from pure conducting polymers have a relatively slow response time (almost 20 minutes), with an irreversible decay in their conductivity. Two methods were proposed to improve the properties of textile-type chemical sensors, namely, doping[225–227] and preparing electrospun nanofibers.[116,117,227–230] After modification, the one-dimensional nanofibers, with a high surface-to-volume ratio and large length-to-diameter ratio, had many more active sites for the adsorption of chemical gases and resulted in more changes to free hole charge carriers, which enhanced the sensitivity. These sensors exhibited a minimum detection limit of 1–5 ppm and a rapid response of less than 1 s, with a relatively slow recovery time of 30 s. The sensors could be used repeatedly and were more sensitive to chemicals than their film counterparts.

Both stability and selectivity are crucial factors for practical applications as chemical sensors. Unfortunately, the performances of the current sensors, which are typically based on conducting polymers, tend to dramatically degrade after a certain period as a result of the de-doping and degeneration of the conductive components. In addition, an ideal chemical sensor should be sensitive to one particular chemical. However, the present chemical sensors are sensitive to many chemicals, and the response to one chemical is easily influenced by the presence of other chemicals. Furthermore, the chemical sensors may be sensitive to the surrounding environment such as the humidity.

5.2.4. Humidity Sensors

Humidity plays a vital role to the survival of animals and plants, human comfort, industrial process control, and high-tech instruments.[231] Thus, the measurement of humidity is significantly important, and fiber-shaped or textile-based sensors for humidity have been constructed, with a focus on portability. The fiber-shaped humidity sensors are mostly built from CNTs. The resistance of this type of sensor increases as the humidity increases because the reversible hygroscopic swelling of the substrate fiber disrupts the electron transport between the CNTs. They were made by coating CNTs onto a fiber substrate by a simple and scalable dip-coating method and dispersing CNTs in polymers to form composite fibers by a melt-spinning process.[232–234] Textile-based humidity sensors can be prepared by coating polymers on commercial fabric with a high strength, flexibility, and high surface area by a simple dip-coating method[224,235] or prepared directly by an electrospinning process.[229,236–240] To further improve their performances, many other materials have been doped into these bare ceramics such as LiCl-[241] and KCl-doped TiO_2 nonwoven fabrics,[242] and LiCl-, KCl-, and Na^+-doped ZnO nonwoven fabrics.[243–245] Dissociated ions other than H^+ and OH^- can also be readily formed in the doped ceramic nanofibers and serve as conductive carriers. The ideal humidity sensor should not only be sensitive to humidity, but also have a high accuracy, good precision, good repeatability, high stability, and short response time. An ultraprecise humidity sensor is still waiting to be developed.

5.2.5. Self-Powering Sensors

Generally, for the various sensors, a power source is inevitable for the measurements, which means that an external power supply has to be integrated into the sensor system.[164,165] Consequently, not only does the manufacturing difficulty and cost of the sensor devices increase, but the comfort of the wearable textiles in terms of flexibility and weight are also greatly affected. Thus, self-powering wearable sensors are in demand. Strain sensors based on piezoelectric materials are one kind of self-powering sensors. The piezoelectric materials can generate a voltage or current in response to an applied force as a consequence of a change in the distance between dipoles within the material.[165] Various inorganic piezoelectric materials such as ZnO, CdS, $BaTiO_3$, $PbTiO_3$, and $PbZrTiO_3$ as well as polymers such as PVDF have been used to fabricate self-powering sensors in response to mechanical stimuli.[79,246,247]

Fiber-shaped sensors of this kind were made from piezoelectric ZnO nanowires to detect pressure and bending motions.[40] However, they still suffered from the drawbacks of stiffness and limited tolerance to strain (less than 5%). Some attempts were made to endow the piezoelectric sensors with stretchability by compositing piezoelectric inorganic materials with an elastic substrate and polymeric additives.[247,248] For example, a $BaTiO_3$ nanowires/poly(vinyl chloride) composite fiber was fabricated through a wet-spinning process. The poly(vinyl alcohol) matrix provided the composite fiber with flexibility to bend at a large angle.[247] The $BaTiO_3$ nanowires were highly aligned in the poly(vinyl chloride) matrix and thus the bending of fingers could be detected through a piezoelectric effect. PVDF and its copolymers constitute one of the most explored families of piezoelectric polymers because of their high flexibility and good processibility compared with piezoelectric inorganic materials. PVDF could be readily made into nonwoven mats by electrospinning; the PVDF nanofibers were simultaneously polarized and highly aligned.[249–251] Thus, the nonwoven mats could be used directly as strain sensors without additional high-voltage polarization and showed high sensitivity.[252] Moreover, they are lightweight, air-permeable, and highly flexible, and thus can be widely used as sensing fabrics.

Self-powering fibers/fabrics that respond to strain or pressure could also be designed based on mechanisms other than the piezoelectric effect.[253–256] For example, based on an electrostatic mechanism, a fiber sensor was fabricated by twisting two cotton fibers, one coated with CNTs while the other was successively coated with CNTs and polytetrafluoroethylene, to form a double-helix configuration.[254] The double-helix cotton fibers were further coiled around a stretchable polymeric fiber substrate. The fiber-shaped sensing device generated electric signals on stretching of the substrate as the double-helix fibers approached each other. This kind of stretchable fiber sensor could be readily woven into commercial textiles to monitor body motions with high stability and durability. Other kinds of self-powering fiber/fabric sensors based on the triboelectric mechanism have also been explored and showed good sensing properties.[255,256]

Although chromatic, deformable, and other functionalities are widely investigated and multifunctional textiles represent a promising direction for the near future, there are limited reports on the introduction of these functionalities to smart electronic textiles that can generate, store, and utilize electricity. This phenomenon may be explained by the fact that the field of electronic textiles started to blossom just a few years ago, and it takes time for progress to be made, although the importance has been well recognized.

6. Conclusions and Outlook

In this Review, we have presented four kinds of smart electronic textiles based on different functionalities, namely, electricity generation, electricity storage, electricity utilization, and their integration. These devices are generally composed of active materials sandwiched between two electrodes, and some of them need electrolytes. The main focus in recent years has been to optimize the materials and structures.

The first important aspect is the preparation of high-performance fiber and textile electrodes. Metal-based fibers and textiles display high electrical conductivities but have low flexibility and can not be stretched. In contrast, polymer-based conductive electrodes show lower electrical conductivities but higher flexibility and stretchability. Although fibers and textiles based on carbon nanomaterials are expected to balance the above properties to more effectively satisfy the electrode applications, a lot of effort is needed to optimize both the preparation and structure.

The second important point is related to coating active materials onto electrodes. A variety of methods, for example, physical deposition, electrochemical processes, and solution coating, have been developed to control the structure and morphology of active layers to improve the electronic performance. However, challenges remain to produce continuous and stable interfaces because of the rough and curved surface compared to planar substrates.

The third important point refers to the fact that the electronic devices often require the use of electrolytes. Gel and solid electrolytes are preferred instead of liquid electrolytes for higher stability in wearable electronics, but the performances need to be increased in future studies.

Although advances are continuing and more prototypes are becoming available, there remains a large gap between the best current textile-type electronics and real applications. Textiles are flexible, deformable, breathable, wearable, comfortable, safe, unobtrusive, and decorative. However, the current textile-shaped electronic devices that can be fabricated on a large scale need to be sealed prior to use, which is not compatible with the above advantages. Therefore, it is necessary to produce electronic building blocks at the fiber level, and then weave the electronic fibers into smart textiles. In this way, the electronic fibers are independent from each other and can be connected in series or parallel. In contrast to conventional chemical fibers, it is difficult to continuously weave electronic fibers by using well-developed textile technologies. A lot of effort is required to develop general and effective weaving methods that are compatible with these functional fibers.

The combination of electricity generation, storage, and utilization and the introduction of other functionalities are promising for smart textiles. Although the integration of electricity generation and storage has been widely investigated, the mismatch between the photoelectric conversion and electrochemical storage parts remains a critical barrier for high performances. For example, the supercapacitor part can be quickly charged to full by the solar cell part in seconds because of the low energy density of the supercapacitor. To this end, the use of a lithium ion battery may represent a general and efficient route to solve the above problem, and should be carefully studied in the future. Although the introduction of other functionalities, such as sensing environmental changes, into the electronic textile has only recently been studied, self-powering sensors have been demonstrated for promising applications in wearable and other related fields. More studies need to be made to extend this important direction.

From a viewpoint of practical application, some critical challenges remain that need to be addressed. Firstly, it is difficult to fabricate highly efficient fiber- and textile-shaped electronic devices on a large scale, as their performances greatly decrease as their lengths are increased from centimeters to meters or even longer. This problem is derived from the relatively low electrical conductivity of the widely explored fiber electrodes based on carbon nanomaterials. Secondly, it is challenging to connect a bunch of fiber electrodes after the fiber-shaped electronic devices are woven into textiles. Thirdly, is the question of whether or not to seal the electronic textiles. They become less stable and even soon fail without sealing, but they cannot effectively display the advantages of the textile structure after sealing. Fourthly, washing the electronic textiles is problematic as they may stop working after contact with water. To this end, we propose coating a thin protecting layer on the surfaces of fiber-shaped devices. Another possibility is that it will not be necessary to wash them if a superhydrophobic layer is coated on the surface. More effort is needed to verify the above hypotheses.

In summary, although a lot of studies are required to optimize the structures and enhance the properties of these smart electronic textiles, they have been demonstrated to be promising for a variety of applications. It is proposed that they may bring a technical revolution to our life in the near future.

Acknowledgements

This work was supported by NSFC (21225417, 51403038), MOST (2011CB932503), STCSM (15XD1500400), China Postdoctoral Science Foundation (2047M560290, 2015T80391), Changjiang Chair Professor Program, the Program for Outstanding Young Scholars from the Organization Department of the CPC Central Committee, and the visiting fund from State Key Laboratory for Modification of Chemical Fibers and Polymer Materials.

How to cite: *Angew. Chem. Int. Ed.* **2016**, *55*, 6140 – 6169
Angew. Chem. **2016**, *128*, 6248 – 6277

[1] R. Kates, W. Clark, R. Corell, J. Hall, C. Jaeger, I. Lowe, J. McCarthy, H. Schellnhuber, B. Bolin, N. Dickson, S. Faucheux, G. Gallopin, A. Grubler, B. Huntley, J. Jager, N. Jodha, R. Kasperson, A. Mabogunje, P. Matson, H. Mooney, B. Moore, T. O'Riordan, U. Svedin, *Science* **2001**, *292*, 641 – 642.
[2] N. Armaroli, V. Balzani, *Angew. Chem. Int. Ed.* **2007**, *46*, 52 – 66; *Angew. Chem.* **2007**, *119*, 52 – 67.
[3] B. Gregg, *J. Phys. Chem. B* **2003**, *107*, 4688 – 4698.
[4] R. Service, *Science* **2003**, *301*, 909 – 911.
[5] X. Fan, F. Wang, Z. Chu, L. Chen, C. Zhang, D. Zou, *Appl. Phys. Lett.* **2007**, *90*, 073501.
[6] X. Fan, Z. Z. Chu, F. Z. Wang, C. Zhang, L. Chen, Y. W. Tang, D. C. Zou, *Adv. Mater.* **2008**, *20*, 592 – 595.
[7] T. Chen, L. Qiu, H. G. Kia, Z. Yang, H. Peng, *Adv. Mater.* **2012**, *24*, 4623 – 4628.
[8] S. Hou, Z. Lv, H. Wu, X. Cai, Z. Chu, Yiliguma, D. Zou, *J. Mater. Chem.* **2012**, *22*, 6549 – 6552.
[9] Z. Yang, H. Sun, T. Chen, L. Qiu, Y. Luo, H. Peng, *Angew. Chem. Int. Ed.* **2013**, *52*, 7545 – 7548; *Angew. Chem.* **2013**, *125*, 7693 – 7696.
[10] T. Chen, L. Qiu, Z. Cai, F. Gong, Z. Yang, Z. Wang, H. Peng, *Nano Lett.* **2012**, *12*, 2568 – 2572.
[11] H. Sun, X. You, J. Deng, X. Chen, Z. Yang, J. Ren, H. Peng, *Adv. Mater.* **2014**, *26*, 2868 – 2873.
[12] H. Li, Z. Yang, L. Qiu, X. Fang, H. Sun, P. Chen, S. Pan, H. Peng, *J. Mater. Chem. A* **2014**, *2*, 3841 – 3846.
[13] B. O'Connor, K. P. Pipe, M. Shtein, *Appl. Phys. Lett.* **2008**, *92*, 193306.
[14] Z. Zhang, Z. Yang, Z. Wu, G. Guan, S. Pan, Y. Zhang, H. Li, J. Deng, B. Sun, H. Peng, *Adv. Energy Mater.* **2014**, *4*, 1301750.
[15] M. R. Lee, R. D. Eckert, K. Forberich, G. Dennler, C. J. Brabec, R. A. Gaudiana, *Science* **2009**, *324*, 232 – 235.
[16] L. Qiu, J. Deng, X. Lu, Z. Yang, H. Peng, *Angew. Chem. Int. Ed.* **2014**, *53*, 10425 – 10428; *Angew. Chem.* **2014**, *126*, 10593 – 10596.
[17] Z. Yang, J. Deng, X. Sun, H. Li, H. Peng, *Adv. Mater.* **2014**, *26*, 2643 – 2647.
[18] H. Li, J. Guo, H. Sun, X. Fang, D. Wang, H. Peng, *ChemNanoMater* **2015**, *1*, 399 – 402.
[19] Z. Zhang, Z. Yang, J. Deng, Y. Zhang, G. Guan, H. Peng, *Small* **2015**, *11*, 675 – 680.
[20] A. Bedeloglu, A. Demir, Y. Bozkurt, N. S. Sariciftci, *Synth. Met.* **2009**, *159*, 2043 – 2048.
[21] S. Lee, Y. Lee, J. Park, D. Choi, *Nano Energy* **2014**, *9*, 88 – 93.
[22] I. A. Sahito, K. C. Sun, A. A. Arbab, M. B. Qadir, S. H. Jeong, *Electrochim. Acta* **2015**, *173*, 164 – 171.
[23] Z. Zhang, X. Li, G. Guan, S. Pan, Z. Zhu, D. Ren, H. Peng, *Angew. Chem. Int. Ed.* **2014**, *53*, 11571 – 11574; *Angew. Chem.* **2014**, *126*, 11755 – 11758.
[24] Y. Chae, J. T. Park, J. K. Koh, J. H. Kim, E. Kim, *Mater. Sci. Eng. B* **2013**, *178*, 1117 – 1123.
[25] M. J. Yun, S. I. Cha, S. H. Seo, H. S. Kim, D. Y. Lee, *Sci. Rep.* **2015**, *5*, 11022.
[26] S. Pan, Z. Yang, P. Chen, J. Deng, H. Li, H. Peng, *Angew. Chem. Int. Ed.* **2014**, *53*, 6110 – 6114; *Angew. Chem.* **2014**, *126*, 6224 – 6228.
[27] R. A. Doyle, V. V. Gridin, *Europhys. Lett.* **1992**, *19*, 423 – 428.
[28] V. Leonov, R. J. M. Vullers, *J. Renewable Sustainable Energy* **2009**, *1*, 062701.
[29] S. J. Kim, J. H. We, B. J. Cho, *Energy Environ. Sci.* **2014**, *7*, 1959 – 1965.
[30] G. Snyder, E. Toberer, *Nat. Mater.* **2008**, *7*, 105 – 114.
[31] J. E. Ni, E. D. Case, K. N. Khabir, R. C. Stewart, C.-I. Wu, T. P. Hogan, E. J. Timm, S. N. Girard, M. G. Kanatzidis, *Mater. Sci. Eng. B* **2010**, *170*, 58 – 66.
[32] C. A. Hewitt, A. B. Kaiser, S. Roth, M. Craps, R. Czerw, D. L. Carroll, *Nano Lett.* **2012**, *12*, 1307 – 1310.
[33] S. L. Kim, K. Choi, A. Tazebay, C. Yu, *ACS Nano* **2014**, *8*, 2377 – 2386.
[34] L. Vladimir, *IEEE Sens. J.* **2013**, *13*, 2284 – 2291.
[35] D. Zabek, J. Taylor, E. L. Boulbar, C. R. Bowen, *Adv. Energy Mater.* **2015**, *5*, 1401891.
[36] J. H. Lee, K. Y. Lee, M. K. Gupta, T. Y. Kim, D. Y. Lee, J. Oh, C. Ryu, W. J. Yoo, C. Y. Kang, S. J. Yoon, J. B. Yoo, S. W. Kim, *Adv. Mater.* **2014**, *26*, 765 – 769.
[37] E. F. Crawley, J. De Luis, *AIAA J.* **1987**, *25*, 1373 – 1385.
[38] S.-E. Park, T. R. Shrout, *J. Appl. Phys.* **1997**, *82*, 1804 – 1811.
[39] Z. L. Wang, J. Song, *Science* **2006**, *312*, 242 – 246.
[40] Y. Qin, X. Wang, Z. L. Wang, *Nature* **2008**, *451*, 809 – 813.
[41] C.-W. Nan, M. I. Bichurin, S. Dong, D. Viehland, G. Srinivasan, *J. Appl. Phys.* **2008**, *103*, 031101.
[42] Y. Qiu, H. Zhang, L. Hu, D. Yang, L. Wang, B. Wang, J. Ji, G. Liu, X. Liu, J. Lin, F. Li, S. Han, *Nanoscale* **2012**, *4*, 6568 – 6573.
[43] Q. Sun, W. Seung, B. J. Kim, S. Seo, S. W. Kim, J. H. Cho, *Adv. Mater.* **2015**, *27*, 3411 – 3417.
[44] L. Gu, N. Cui, L. Cheng, Q. Xu, S. Bai, M. Yuan, W. Wu, J. Liu, Y. Zhao, F. Ma, Y. Qin, Z. L. Wang, *Nano Lett.* **2013**, *13*, 91 – 94.
[45] M. Lee, C. Y. Chen, S. Wang, S. N. Cha, Y. J. Park, J. M. Kim, L. J. Chou, Z. L. Wang, *Adv. Mater.* **2012**, *24*, 1759 – 1764.
[46] R. Yang, Y. Qin, L. Dai, Z. L. Wang, *Nat. Nanotechnol.* **2009**, *4*, 34 – 39.
[47] E. Nilsson, A. Lund, C. Jonasson, C. Johansson, B. Hagström, *Sens. Actuators A* **2013**, *201*, 477 – 486.
[48] X. Li, Z. Lin, G. Cheng, X. Wen, Y. Liu, S. Niu, Z. Wang, *ACS Nano* **2014**, *8*, 10674 – 10681.
[49] S. Bai, L. Zhang, Q. Xu, Y. Zheng, Y. Qin, Z. L. Wang, *Nano Energy* **2013**, *2*, 749 – 753.
[50] N. Soin, T. H. Shah, S. C. Anand, J. Geng, W. Pornwannachai, P. Mandal, D. Reid, S. Sharma, R. L. Hadimani, D. V. Bayramol, E. Siores, *Energy Environ. Sci.* **2014**, *7*, 1670 – 1679.
[51] A. Khan, M. A. Abbasi, M. Hussain, Z. H. Ibupoto, J. Wissting, O. Nur, M. Willander, *Appl. Phys. Lett.* **2012**, *101*, 193506.
[52] A. Khan, M. Hussain, O. Nur, M. Willander, *Chem. Phys. Lett.* **2014**, *612*, 62 – 67.
[53] K. H. Kim, K. Y. Lee, J. S. Seo, B. Kumar, S. W. Kim, *Small* **2011**, *7*, 2577 – 2580.
[54] M. G. Kim, J. Cho, *Adv. Funct. Mater.* **2009**, *19*, 1497 – 1514.
[55] J. Liu, X. W. Liu, *Adv. Mater.* **2012**, *24*, 4097 – 4111.
[56] H. Lin, L. Li, J. Ren, Z. Cai, L. Qiu, Z. Yang, H. Peng, *Sci. Rep.* **2013**, *3*, 1353.
[57] M. Armand, J. Tarascon, *Nature* **2008**, *451*, 652 – 657.
[58] J. Ren, Y. Zhang, W. Bai, X. Chen, Z. Zhang, X. Fang, W. Weng, Y. Wang, H. Peng, *Angew. Chem. Int. Ed.* **2014**, *53*, 7864 – 7869; *Angew. Chem.* **2014**, *126*, 7998 – 8003.
[59] J. Kim, A. Manthiram, *Nature* **1997**, *390*, 265 – 267.
[60] K. Nam, D. Kim, P. Yoo, C. Chiang, N. Meethong, P. Hammond, Y. Chiang, A. Belcher, *Science* **2006**, *312*, 885 – 888.
[61] X. Fang, H. Peng, *Small* **2015**, *11*, 1488 – 1511.
[62] L. Ji, Z. Lin, M. Alcoutlabi, X. Zhang, *Energy Environ. Sci.* **2011**, *4*, 2682 – 2699.
[63] Y. H. Kwon, S. W. Woo, H. R. Jung, H. K. Yu, K. Kim, B. H. Oh, S. Ahn, S. Y. Lee, S. W. Song, J. Cho, H. C. Shin, J. Y. Kim, *Adv. Mater.* **2012**, *24*, 5192 – 5197.
[64] H. Lin, W. Weng, J. Ren, L. Qiu, Z. Zhang, P. Chen, X. Chen, J. Deng, Y. Wang, H. Peng, *Adv. Mater.* **2014**, *26*, 1217 – 1222.
[65] C.-F. Sun, H. Zhu, E. B. Baker III, M. Okada, J. Wan, A. Ghemes, Y. Inoue, L. Hu, Y. Wang, *Nano Energy* **2013**, *2*, 987 – 994.
[66] W. Weng, Q. Sun, Y. Zhang, H. Lin, J. Ren, X. Lu, M. Wang, H. Peng, *Nano Lett.* **2014**, *14*, 3432 – 3438.
[67] Y. Zhang, W. Bai, J. Ren, W. Weng, H. Lin, Z. Zhang, H. Peng, *J. Mater. Chem. A* **2014**, *2*, 11054 – 11059.

[68] Y. Zhang, W. Bai, X. Cheng, J. Ren, W. Weng, P. Chen, X. Fang, Z. Zhang, H. Peng, *Angew. Chem. Int. Ed.* **2014**, *53*, 14564 – 14568; *Angew. Chem.* **2014**, *126*, 14792 – 14796.

[69] Y. H. Lee, J. S. Kim, J. Noh, I. Lee, H. J. Kim, S. Choi, J. Seo, S. Jeon, T. S. Kim, J. Y. Lee, J. W. Choi, *Nano Lett.* **2013**, *13*, 5753 – 5761.

[70] B. Liu, J. Zhang, X. Wang, G. Chen, D. Chen, C. Zhou, G. Shen, *Nano Lett.* **2012**, *12*, 3005 – 3011.

[71] L. Gao, F. Qu, X. Wu, *J. Mater. Chem. A* **2014**, *2*, 7367 – 7372.

[72] M.-S. Balogun, M. Yu, Y. Huang, C. Li, P. Fang, Y. Liu, X. Lu, Y. Tong, *Nano Energy* **2015**, *11*, 348 – 355.

[73] W. Li, X. Wang, B. Liu, S. Luo, Z. Liu, X. Hou, Q. Xiang, D. Chen, G. Shen, *Chem. Eur. J.* **2013**, *19*, 8650 – 8656.

[74] L. Shen, B. Ding, P. Nie, G. Cao, X. Zhang, *Adv. Energy Mater.* **2013**, *3*, 1484 – 1489.

[75] A. G. Pandolfo, A. F. Hollenkamp, *J. Power Sources* **2006**, *157*, 11 – 27.

[76] R. Kötz, M. Carlen, *Electrochim. Acta* **2000**, *45*, 2483 – 2498.

[77] P. Simon, Y. Gogotsi, *Nat. Mater.* **2008**, *7*, 845 – 854.

[78] G. A. Snook, P. Kao, A. S. Best, *J. Power Sources* **2011**, *196*, 1 – 12.

[79] Y. Fu, X. Cai, H. Wu, Z. Lv, S. Hou, M. Peng, X. Yu, D. Zou, *Adv. Mater.* **2012**, *24*, 5713 – 5718.

[80] N. Liu, W. Ma, J. Tao, X. Zhang, J. Su, L. Li, C. Yang, Y. Gao, D. Golberg, Y. Bando, *Adv. Mater.* **2013**, *25*, 4925 – 4931.

[81] K. Jost, D. Stenger, C. R. Perez, J. K. McDonough, K. Lian, Y. Gogotsi, G. Dion, *Energy Environ. Sci.* **2013**, *6*, 2698 – 2705.

[82] D. Harrison, F. Qiu, J. Fyson, Y. Xu, P. Evans, D. Southee, *Phys. Chem. Chem. Phys.* **2013**, *15*, 12215 – 12219.

[83] J. Ren, W. Bai, G. Guan, Y. Zhang, H. Peng, *Adv. Mater.* **2013**, *25*, 5965 – 5970.

[84] Z. Cai, L. Li, J. Ren, L. Qiu, H. Lin, H. Peng, *J. Mater. Chem. A* **2013**, *1*, 258 – 261.

[85] S. Aboutalebi, R. Jalili, D. Esrafilzadeh, M. Salari, Z. Gholamvand, S. Yamini, K. Konstantinov, R. Shepherd, J. Chen, S. Moulton, *ACS Nano* **2014**, *8*, 2456 – 2466.

[86] B. Liu, B. Liu, X. Wang, D. Chen, Z. Fan, G. Shen, *Nano Energy* **2014**, *10*, 99 – 107.

[87] L. Kou, T. Huang, B. Zheng, Y. Han, X. Zhao, K. Gopalsamy, H. Sun, C. Gao, *Nat. Commun.* **2014**, *5*, 3754.

[88] Q. Meng, K. Wang, W. Guo, J. Fang, Z. Wei, X. She, *Small* **2014**, *10*, 3187 – 3193.

[89] X. Chen, L. Qiu, J. Ren, G. Guan, H. Lin, Z. Zhang, P. Chen, Y. Wang, H. Peng, *Adv. Mater.* **2013**, *25*, 6436 – 6441.

[90] X. Chen, H. Lin, J. Deng, Y. Zhang, X. Sun, P. Chen, X. Fang, Z. Zhang, G. Guan, H. Peng, *Adv. Mater.* **2014**, *26*, 8126 – 8132.

[91] X. Wang, B. Liu, R. Liu, Q. Wang, X. Hou, D. Chen, R. Wang, G. Shen, *Angew. Chem. Int. Ed.* **2014**, *53*, 1849 – 1853; *Angew. Chem.* **2014**, *126*, 1880 – 1884.

[92] Z. Zhang, J. Deng, X. Li, Z. Yang, S. He, X. Chen, G. Guan, J. Ren, H. Peng, *Adv. Mater.* **2015**, *27*, 356 – 362.

[93] S. Pan, J. Deng, G. Guan, Y. Zhang, P. Chen, J. Ren, H. Peng, *J. Mater. Chem. A* **2015**, *3*, 6286 – 6290.

[94] Z. Yang, J. Deng, X. Chen, J. Ren, H. Peng, *Angew. Chem. Int. Ed.* **2013**, *52*, 13453 – 13457; *Angew. Chem.* **2013**, *125*, 13695 – 13699.

[95] L. Hu, M. Pasta, F. L. Mantia, L. Cui, S. Jeong, H. D. Deshazer, J. W. Choi, S. M. Han, Y. Cui, *Nano Lett.* **2010**, *10*, 708 – 714.

[96] L. Hu, W. Chen, X. Xie, N. Liu, Y. Yang, H. Wu, Y. Yao, M. Pasta, H. N. Alshareef, Y. Cui, *ACS Nano* **2011**, *5*, 8904 – 8913.

[97] W. Liu, X. Yan, J. Lang, C. Peng, Q. Xue, *J. Mater. Chem.* **2012**, *22*, 17245 – 17253.

[98] C. Shi, Q. Zhao, H. Li, Z.-M. Liao, D. Yu, *Nano Energy* **2014**, *6*, 82 – 91.

[99] C. Zhou, J. Liu, *Nanotechnology* **2014**, *25*, 035402.

[100] C. Meng, C. Liu, L. Chen, C. Hu, S. Fan, *Nano Lett.* **2010**, *10*, 4025 – 4031.

[101] L. Du, P. Yang, X. Yu, P. Liu, J. Song, W. Mai, *J. Mater. Chem. A* **2014**, *2*, 17561 – 17567.

[102] S. Pan, H. Lin, J. Deng, P. Chen, X. Chen, Z. Yang, H. Peng, *Adv. Energy Mater.* **2015**, *5*, 1401438.

[103] J. Jensen, M. Hösel, A. L. Dyer, F. C. Krebs, *Adv. Funct. Mater.* **2015**, *25*, 2073 – 2090.

[104] P. M. Beaujuge, J. R. Reynolds, *Chem. Rev.* **2010**, *110*, 268 – 320.

[105] W. M. Kline, R. G. Lorenzini, G. A. Sotzing, *Color. Technol.* **2014**, *130*, 73 – 80.

[106] K. Wang, H. Wu, Y. Meng, Y. Zhang, Z. Wei, *Energy Environ. Sci.* **2012**, *5*, 8384 – 8389.

[107] E. O. Polat, O. Balci, C. Kocabas, *Sci. Rep.* **2014**, *4*, 6484.

[108] J. Jensen, F. C. Krebs, *Adv. Mater.* **2014**, *26*, 7231 – 7234.

[109] X. Chen, H. Lin, P. Chen, G. Guan, J. Deng, H. Peng, *Adv. Mater.* **2014**, *26*, 4444 – 4449.

[110] C. Yan, W. Kang, J. Wang, M. Cui, X. Wang, C. Y. Foo, K. J. Chee, P. S. Lee, *ACS Nano* **2014**, *8*, 316 – 322.

[111] V. K. Thakur, G. Ding, J. Ma, P. S. Lee, X. Lu, *Adv. Mater.* **2012**, *24*, 4071 – 4096.

[112] H. Peng, X. Sun, F. Cai, X. Chen, Y. Zhu, G. Liao, D. Chen, Q. Li, Y. Lu, Y. Zhu, Q. Jia, *Nat. Nanotechnol.* **2009**, *4*, 738 – 741.

[113] H. Guo, J. Zhang, D. Porter, H. Peng, D. W. P. M. Lowik, Y. Wang, Z. Zhang, X. Chen, Z. Shao, *Chem. Sci.* **2014**, *5*, 4189 – 4195.

[114] K. Li, Q. Zhang, H. Wang, Y. Li, *ACS Appl. Mater. Interfaces* **2014**, *6*, 13043 – 13050.

[115] A. Laforgue, G. Rouget, S. Dubost, M. F. Champagne, L. Robitaille, *ACS Appl. Mater. Interfaces* **2012**, *4*, 3163 – 3168.

[116] Y. Ding, M. A. Invernale, G. A. Sotzing, *ACS Appl. Mater. Interfaces* **2010**, *2*, 1588 – 1593.

[117] M. A. Invernale, Y. Ding, G. A. Sotzing, *ACS Appl. Mater. Interfaces* **2010**, *2*, 296 – 300.

[118] A. Laforgue, *J. Mater. Chem.* **2010**, *20*, 8233 – 8235.

[119] M. A. Invernale, Y. Ding, G. A. Sotzing, *Color. Technol.* **2011**, *127*, 167 – 172.

[120] S. M. Donovan, S. D. Hartford, M. L. Kvernmo, A. A. Owings, B. W. Wilkins, U.S. Patent, No. 8,650,764, **2014**.

[121] J. A. Kerszulis, K. E. Johnson, M. Kuepfert, D. Khoshabo, A. L. Dyer, J. R. Reynolds, *J. Mater. Chem. C* **2015**, *3*, 3211 – 3218.

[122] A. Kraft, A. C. Grimsdale, A. B. Holmes, *Angew. Chem. Int. Ed.* **1998**, *37*, 402 – 428; *Angew. Chem.* **1998**, *110*, 416 – 443.

[123] Z. Yu, Q. Zhang, L. Li, Q. Chen, X. Niu, J. Liu, Q. Pei, *Adv. Mater.* **2011**, *23*, 664 – 668.

[124] Z. Yu, X. Niu, Z. Liu, Q. Pei, *Adv. Mater.* **2011**, *23*, 3989 – 3994.

[125] S. Kim, H.-J. Kwon, S. Lee, H. Shim, Y. Chun, W. Choi, J. Kwack, D. Han, M. Song, S. Kim, S. Mohammadi, I. Kee, S. Y. Lee, *Adv. Mater.* **2011**, *23*, 3511 – 3516.

[126] T. Sekitani, H. Nakajima, H. Maeda, T. Fukushima, T. Aida, K. Hata, T. Someya, *Nat. Mater.* **2009**, *8*, 494 – 499.

[127] T.-H. Han, Y. Lee, M.-R. Choi, S.-H. Woo, S.-H. Bae, B. H. Hong, J.-H. Ahn, T.-W. Lee, *Nat. Photonics* **2012**, *6*, 105 – 110.

[128] J. Liang, L. Li, X. Niu, Z. Yu, Q. Pei, *Nat. Photonics* **2013**, *7*, 817 – 824.

[129] M. S. White, M. Kaltenbrunner, E. D. Glowacki, K. Gutnichenko, G. Kettlgruber, I. Graz, S. Aazou, C. Ulbricht, D. A. M. Egbe, M. C. Miron, Z. Major, M. C. Scharber, T. Sekitani, T. Someya, S. Bauer, N. S. Sariciftci, *Nat. Photonics* **2013**, *7*, 811 – 816.

[130] M. Vosgueritchian, J. B. H. Tok, Z. Bao, *Nat. Photonics* **2013**, *7*, 769 – 771.

[131] B. O'Connor, K. H. An, Y. Zhao, K. P. Pipe, M. Shtein, *Adv. Mater.* **2007**, *19*, 3897 – 3900.

[132] H. Yang, C. R. Lightner, L. Dong, *ACS Nano* **2012**, *6*, 622 – 628.

[133] Z. Zhang, K. Guo, Y. Li, X. Li, G. Guan, H. Li, Y. Luo, F. Zhao, Q. Zhang, B. Wei, Q. Pei, H. Peng, *Nat. Photonics* **2015**, *9*, 233 – 238.

[134] T. Dias, R. Monaragala, *Text. Res. J.* **2012**, *82*, 1164 – 1176.

[135] B. Hu, D. Li, O. Ala, P. Manandhar, Q. Fan, D. Kasilingam, P. D. Calvert, *Adv. Funct. Mater.* **2011**, *21*, 305 – 311.
[136] B. Hu, D. Li, P. Manandharm, Q. Fan, D. Kasilingam, P. Calvert, *J. Mater. Chem.* **2012**, *22*, 1598 – 1605.
[137] W. Kim, S. Kwon, S.-M. Lee, J. Y. Kim, Y. Han, E. Kim, K. C. Choi, S. Park, B.-C. Park, *Org. Electron.* **2013**, *14*, 3007 – 3013.
[138] K. Cherenack, L. van Pieterson, *J. Appl. Phys.* **2012**, *112*, 091301.
[139] R. H. Baughman, C. Cui, A. A. Zakhidov, Z. Iqbal, J. N. Barisci, G. M. Spinks, G. G. Wallace, A. Mazzoldi, D. De Rossi, A. G. Rinzler, O. Jaschinski, S. Roth, M. Kertesz, *Science* **1999**, *284*, 1340 – 1344.
[140] L. Viry, C. Mercader, P. Miaudet, C. Zakri, A. Derre, A. Kuhn, M. Maugey, P. Poulin, *J. Mater. Chem.* **2010**, *20*, 3487 – 3495.
[141] Y. Yun, V. Shanov, Y. Tu, M. J. Schulz, S. Yarmolenko, S. Neralla, J. Sankar, S. Subramaniam, *Nano Lett.* **2006**, *6*, 689 – 693.
[142] T. Mirfakhrai, J. Oh, M. Kozlov, E. C. W. Fok, M. Zhang, S. Fang, R. H. Baughman, J. D. W. Madden, *Smart Mater. Struct.* **2007**, *16*, S243 – S249.
[143] J. Foroughi, G. M. Spinks, G. G. Wallace, J. Oh, M. E. Kozlov, S. Fang, T. Mirfakhrai, J. D. W. Madden, M. K. Shin, S. J. Kim, R. H. Baughman, *Science* **2011**, *334*, 494 – 497.
[144] J. A. Lee, Y. T. Kim, G. M. Spinks, D. Suh, X. Lepró, M. D. Lima, R. H. Baughman, S. J. Kim, *Nano Lett.* **2014**, *14*, 2664 – 2669.
[145] W. Guo, C. Liu, F. Zhao, X. Sun, Z. Yang, T. Chen, X. Chen, L. Qiu, X. Hu, H. Peng, *Adv. Mater.* **2012**, *24*, 5379 – 5384.
[146] P. Chen, Y. Xu, S. He, X. Sun, W. Guo, Z. Zhang, L. Qiu, J. Li, D. Chen, H. Peng, *Adv. Mater.* **2015**, *27*, 1042 – 1047.
[147] F. Meng, X. Zhang, R. Li, J. Zhao, X. Xuan, X. Wang, J. Zou, Q. Li, *Adv. Mater.* **2014**, *26*, 2480 – 2485.
[148] J. Yuan, P. Poulin, *Science* **2014**, *343*, 845 – 846.
[149] P. Chen, S. He, Y. Xu, X. Sun, H. Peng, *Adv. Mater.* **2015**, *27*, 4982 – 4988.
[150] M. D. Lima, N. Li, M. J. de Andrade, S. Fang, J. Oh, G. M. Spinks, M. E. Kozlov, C. S. Haines, D. Suh, J. Foroughi, S. J. Kim, Y. Chen, T. Ware, M. K. Shin, L. D. Machado, A. F. Fonseca, J. D. W. Madden, W. E. Voit, D. S. Galvão, R. H. Baughman, *Science* **2012**, *338*, 928 – 932.
[151] Y. Shang, X. He, C. Wang, L. Zhu, Q. Peng, E. Shi, S. Wu, Y. Yang, W. Xu, R. Wang, S. Du, A. Cao, Y. Li, *Adv. Eng. Mater.* **2015**, *17*, 14 – 20.
[152] Y. Liu, H. Lv, X. Lan, J. Leng, S. Du, *Compos. Sci. Technol.* **2009**, *69*, 2064 – 2068.
[153] J. Hu, S. Chen, *J. Mater. Chem.* **2010**, *20*, 3346 – 3355.
[154] Q. Meng, J. Hu, L. Yeung, *Smart Mater. Struct.* **2007**, *16*, 830 – 836.
[155] T. Chen, L. Qiu, Z. Yang, Z. Cai, J. Ren, H. Li, H. Lin, X. Sun, H. Peng, *Angew. Chem. Int. Ed.* **2012**, *51*, 11977 – 11980; *Angew. Chem.* **2012**, *124*, 12143 – 12146.
[156] X. Chen, H. Sun, Z. Yang, G. Guan, Z. Zhang, L. Qiu, H. Peng, *J. Mater. Chem. A* **2014**, *2*, 1897 – 1902.
[157] Z. Zhang, X. Chen, P. Chen, G. Guan, L. Qiu, H. Lin, Z. Yang, W. Bai, Y. Luo, H. Peng, *Adv. Mater.* **2014**, *26*, 466 – 470.
[158] Z. Yang, J. Deng, H. Sun, J. Ren, S. Pan, H. Peng, *Adv. Mater.* **2014**, *26*, 7038 – 7042.
[159] H. Sun, X. You, J. Deng, X. Chen, Z. Yang, P. Chen, X. Fang, H. Peng, *Angew. Chem. Int. Ed.* **2014**, *53*, 6664 – 6668; *Angew. Chem.* **2014**, *126*, 6782 – 6786.
[160] R. Song, H. Jin, X. Li, L. Fei, Y. Zhao, H. Huang, H. L.-W. Chan, Y. Wang, Y. Chai, *J. Mater. Chem. A* **2015**, *3*, 14963 – 14970.
[161] S. Wang, Z.-H. Lin, S. Niu, L. Lin, Y. Xie, K. C. Pradel, Z. L. Wang, *ACS Nano* **2013**, *7*, 11263 – 11271.
[162] M. Stoppa, A. Chiolerio, *Sensors* **2014**, *14*, 11957 – 11992.
[163] S. Ma, Y. Wang, Z. Min, L. Zhong, *Polym. Int.* **2013**, *62*, 983 – 990.
[164] W. Zeng, L. Shu, Q. Li, S. Chen, F. Wang, X. M. Tao, *Adv. Mater.* **2014**, *26*, 5310 – 5336.
[165] M. L. Hammock, A. Chortos, B. C. K. Tee, J. B. H. Tok, Z. Bao, *Adv. Mater.* **2013**, *25*, 5997 – 6038.
[166] W. P. Eaton, J. H. Smith, *Smart Mater. Struct.* **1997**, *6*, 530 – 539.
[167] J. Wu, D. Zhou, C. O. Too, G. G. Wallace, *Synth. Met.* **2005**, *155*, 698 – 701.
[168] P. Xue, X. M. Tao, H. Y. Tsang, *Appl. Surf. Sci.* **2007**, *253*, 3387 – 3392.
[169] P. Xue, J. Wang, X. Tao, *High Perform. Polym.* **2014**, *26*, 364 – 370.
[170] M. Z. Seyedin, J. M. Razal, P. C. Innis, G. G. Wallace, *Adv. Funct. Mater.* **2014**, *24*, 2957 – 2966.
[171] S. Lee, S. Shin, S. Lee, J. Seo, J. Lee, S. Son, H. J. Cho, H. Algadi, S. Al-Sayari, D. E. Kim, T. Lee, *Adv. Funct. Mater.* **2015**, *25*, 3114 – 3121.
[172] C. Yan, J. Wang, W. Kang, M. Cui, X. Wang, C. Y. Foo, K. J. Chee, P. S. Lee, *Adv. Mater.* **2014**, *26*, 2022 – 2027.
[173] N. P. Dasgupta, J. Sun, C. Liu, S. Brittman, S. C. Andrews, J. Lim, H. Gao, R. Yan, P. Yang, *Adv. Mater.* **2014**, *26*, 2137 – 2184.
[174] J. Zhou, E. Q. Li, R. P. Li, X. Z. Xu, I. A. Ventura, A. Moussawi, D. H. Anjum, M. N. Hedhili, D. M. Smilgies, G. Lubineau, S. T. Thoroddsen, *J. Mater. Chem. C* **2015**, *3*, 2528 – 2538.
[175] M. F. De Volder, S. H. Tawfick, R. H. Baughman, A. J. Hart, *Science* **2013**, *339*, 535 – 539.
[176] K. Koziol, J. Vilatela, A. Moisala, M. Motta, P. Cunniff, M. Sennett, A. Windle, *Science* **2007**, *318*, 1892 – 1895.
[177] W. Lu, M. Zu, J. H. Byun, B. S. Kim, T. W. Chou, *Adv. Mater.* **2012**, *24*, 1805 – 1833.
[178] Y. Shang, X. He, Y. Li, L. Zhang, Z. Li, C. Ji, E. Shi, P. Li, K. Zhu, Q. Peng, C. Wang, X. Zhang, R. Wang, J. Wei, K. Wang, H. Zhu, D. Wu, A. Cao, *Adv. Mater.* **2012**, *24*, 2896 – 2900.
[179] Y. Y. Shang, Y. B. Li, X. D. He, S. Y. Du, L. H. Zhang, E. Z. Shi, S. T. Wu, Z. Li, P. X. Li, J. Q. Wei, K. L. Wang, H. W. Zhu, D. H. Wu, A. Y. Cao, *ACS Nano* **2013**, *7*, 1446 – 1453.
[180] Y. B. Li, Y. Y. Shang, X. D. He, Q. Y. Peng, S. Y. Du, E. Z. Shi, S. T. Wu, Z. Li, P. X. Li, A. Y. Cao, *ACS Nano* **2013**, *7*, 8128 – 8135.
[181] J. K. Sun, Y. H. Li, Q. Y. Peng, S. C. Hou, D. C. Zou, Y. Y. Shang, Y. B. Li, P. X. Li, Q. J. Du, Z. H. Wang, Y. Z. Xia, L. H. Xia, X. L. Li, A. Y. Cao, *ACS Nano* **2013**, *7*, 10225 – 10232.
[182] A. Ehrmann, F. Heimlich, A. Brucken, M. Weber, R. Haug, *Text. Res. J.* **2014**, *84*, 2006 – 2012.
[183] C. Zysset, T. Kinkeldei, N. Munzenrieder, L. Petti, G. Salvatore, G. Troster, *Text. Res. J.* **2013**, *83*, 1130 – 1142.
[184] T. W. Shyr, J. W. Shie, Y. E. Jhuang, *Sensors* **2011**, *11*, 1693 – 1705.
[185] T. Yamashita, S. Takamatsu, K. Miyake, T. Itoh, *Sens. Actuators A* **2013**, *195*, 213 – 218.
[186] O. Atalay, W. R. Kennon, *Sensors* **2014**, *14*, 4712 – 4730.
[187] T. W. Shyr, J. W. Shie, C. H. Jiang, J. J. Li, *Sensors* **2014**, *14*, 4050 – 4059.
[188] E. P. Scilingo, F. Lorussi, A. Mazzoldi, D. De Rossi, *IEEE Sens. J.* **2003**, *3*, 460 – 467.
[189] F. Lorussi, W. Rocchia, E. P. Scilingo, A. Tognetti, D. De Rossi, *IEEE Sens. J.* **2004**, *4*, 807 – 818.
[190] T. E. Campbell, B. J. Munro, G. G. Wallace, J. R. Steele, *J. Biomech.* **2007**, *40*, 3056 – 3059.
[191] Y. Li, X. Y. Cheng, M. Y. Leung, J. Tsang, X. M. Tao, M. C. W. Yuen, *Synth. Met.* **2005**, *155*, 89 – 94.
[192] A. Greiner, J. H. Wendorff, *Angew. Chem. Int. Ed.* **2007**, *46*, 5670 – 5703; *Angew. Chem.* **2007**, *119*, 5770 – 5805.
[193] S. Agarwal, A. Greiner, J. H. Wendorff, *Prog. Polym. Sci.* **2013**, *38*, 963 – 991.

[194] D. Li, Y. N. Xia, *Adv. Mater.* **2004**, *16*, 1151 – 1170.
[195] B. Sun, Y.-Z. Long, Z.-J. Chen, S.-L. Liu, H.-D. Zhang, J.-C. Zhang, W.-P. Han, *J. Mater. Chem. C* **2014**, *2*, 1209 – 1219.
[196] N. Liu, G. Fang, J. Wan, H. Zhou, H. Long, X. Zhao, *J. Mater. Chem.* **2011**, *21*, 18962 – 18966.
[197] L. Cai, L. Song, P. Luan, Q. Zhang, N. Zhang, Q. Gao, D. Zhao, X. Zhang, M. Tu, F. Yang, W. Zhou, Q. Fan, J. Luo, W. Zhou, P. M. Ajayan, S. Xie, *Sci. Rep.* **2013**, *3*, 3048.
[198] J. T. Han, S. Choi, J. I. Jang, S. K. Seol, J. S. Woo, H. J. Jeong, S. Y. Jeong, K. J. Baeg, G. W. Lee, *Sci. Rep.* **2015**, *5*, 9300.
[199] S. Takamatsu, T. Kobayashi, N. Shibayama, K. Miyake, T. Itoh, *Sens. Actuators A* **2012**, *184*, 57 – 63.
[200] A. Frutiger, J. T. Muth, D. M. Vogt, Y. Menguc, A. Campo, A. D. Valentine, C. J. Walsh, J. A. Lewis, *Adv. Mater.* **2015**, *27*, 2440 – 2446.
[201] J. Lee, H. Kwon, J. Seo, S. Shin, J. H. Koo, C. Pang, S. Son, J. H. Kim, Y. H. Jang, D. E. Kim, T. Lee, *Adv. Mater.* **2015**, *27*, 2433 – 2439.
[202] H. B. Muhammad, C. Recchiuto, C. M. Oddo, L. Beccai, C. J. Anthony, M. J. Adams, M. C. Carrozza, M. C. L. Ward, *Microelectron. Eng.* **2011**, *88*, 1811 – 1813.
[203] L. Viry, A. Levi, M. Totaro, A. Mondini, V. Mattoli, B. Mazzolai, L. Beccai, *Adv. Mater.* **2014**, *26*, 2659 – 2664.
[204] J. Meyer, B. Arnrich, J. Schumm, G. Troster, *IEEE Sens. J.* **2010**, *10*, 1391 – 1398.
[205] S. Takamatsu, T. Yamashita, T. Imai, T. Itoh, *Sens. Actuators A* **2014**, *220*, 153 – 158.
[206] M. D. Husain, R. Kennon, T. Dias, *J. Ind. Text.* **2014**, *44*, 398 – 417.
[207] D. H. Kim, N. S. Lu, R. Ghaffari, Y. S. Kim, S. P. Lee, L. Z. Xu, J. A. Wu, R. H. Kim, J. Z. Song, Z. J. Liu, J. Viventi, B. de Graff, B. Elolampi, M. Mansour, M. J. Slepian, S. Hwang, J. D. Moss, S. M. Won, Y. G. Huang, B. Litt, J. A. Rogers, *Nat. Mater.* **2011**, *10*, 316 – 323.
[208] K. Cherenack, C. Zysset, T. Kinkeldei, N. Munzenrieder, G. Troster, *Adv. Mater.* **2010**, *22*, 5178 – 5182.
[209] C. Zhang, C.-A. Ma, P. Wang, M. Sumita, *Carbon* **2005**, *43*, 2544 – 2553.
[210] R.-C. Zhuang, T. T. L. Doan, J.-W. Liu, J. Zhang, S.-L. Gao, E. Mäder, *Carbon* **2011**, *49*, 2683 – 2692.
[211] M. Sibinski, M. Jakubowska, M. Sloma, *Sensors* **2010**, *10*, 7934 – 7946.
[212] N. J. Blasdel, E. K. Wujcik, J. E. Carletta, K. S. Lee, C. N. Monty, *IEEE Sens. J.* **2015**, *15*, 300 – 306.
[213] J. Jeon, H. B. Lee, Z. Bao, *Adv. Mater.* **2013**, *25*, 850 – 855.
[214] N. T. Tien, S. Jeon, D. I. Kim, T. Q. Trung, M. Jang, B. U. Hwang, K. E. Byun, J. Bae, E. Lee, J. B. Tok, Z. Bao, N. E. Lee, J. J. Park, *Adv. Mater.* **2014**, *26*, 796 – 804.
[215] I. Graz, M. Krause, S. Bauer-Gogonea, S. Bauer, S. P. Lacour, B. Ploss, M. Zirkl, B. Stadlober, S. Wagner, *J. Appl. Phys.* **2009**, *106*, 034503.
[216] C. Hou, H. Wang, Q. Zhang, Y. Li, M. Zhu, *Adv. Mater.* **2014**, *26*, 5018 – 5024.
[217] K. Kolev, C. Popov, T. Petkova, P. Petkov, I. N. Mihailescu, J. P. Reithmaier, *Sens. Actuators B* **2009**, *143*, 395 – 399.
[218] J. D. W. Madden, N. A. Vandesteeg, P. A. Anquetil, P. G. A. Madden, A. Takshi, R. Z. Pytel, S. R. Lafontaine, P. A. Wieringa, I. W. Hunter, *IEEE J. Oceanic Eng.* **2004**, *29*, 706 – 728.
[219] J. Kong, N. R. Franklin, C. Zhou, M. G. Chapline, S. Peng, K. Cho, H. Dai, *Science* **2000**, *287*, 622 – 625.
[220] J. Yun, H.-I. Kim, Y.-S. Lee, *J. Mater. Sci.* **2013**, *48*, 8320 – 8328.
[221] J. Kim, S. H. Lee, S.-J. Park, Y.-S. Lee, *Res. Chem. Intermed.* **2014**, *40*, 2571 – 2581.
[222] S. Shao, Y. Huang, S. Tao, *IEEE Sens. J.* **2014**, *14*, 847 – 852.
[223] W. Zhang, Y. Y. Tan, C. Wu, S. R. P. Silva, *Particuology* **2012**, *10*, 517 – 521.
[224] G. E. Collins, L. J. Buckley, *Synth. Met.* **1996**, *78*, 93 – 101.
[225] D. Kincal, A. Kumar, A. D. Child, J. R. Reynolds, *Synth. Met.* **1998**, *92*, 53 – 56.
[226] K. H. Hong, K. W. Oh, T. J. Kang, *J. Appl. Polym. Sci.* **2004**, *92*, 37 – 42.
[227] G. Jin, J. Norrish, C. Too, G. Wallace, *Curr. Appl. Phys.* **2004**, *4*, 366 – 369.
[228] O. S. Kwon, E. Park, O. Y. Kweon, S. J. Park, J. Jang, *Talanta* **2010**, *82*, 1338 – 1343.
[229] K. Low, C. B. Horner, C. Li, G. Ico, W. Bosze, N. V. Myung, J. Nam, *Sens. Actuators B* **2015**, *207*, 235 – 242.
[230] S. Ji, Y. Li, M. Yang, *Sens. Actuators B* **2008**, *133*, 644 – 649.
[231] E. Traversa, *Sens. Actuators B* **1995**, *23*, 135 – 136.
[232] B. S. Shim, W. Chen, C. Doty, C. Xu, N. A. Kotov, *Nano Lett.* **2008**, *8*, 4151 – 4157.
[233] S.-l. Gao, R.-C. Zhuang, J. Zhang, J.-W. Liu, E. Mäder, *Adv. Funct. Mater.* **2010**, *20*, 1885 – 1893.
[234] E. Devaux, C. Aubry, C. Campagne, M. Rochery, *J. Eng. Fibers Fabr.* **2011**, *6*, 13 – 24.
[235] W. A. Daoud, J. H. Xin, Y. S. Szeto, *Sens. Actuators B* **2005**, *109*, 329 – 333.
[236] N. Horzum, D. Tascioglu, S. Okur, M. M. Demir, *Talanta* **2011**, *85*, 1105 – 1111.
[237] Y. He, T. Zhang, W. Zheng, R. Wang, X. Liu, Y. Xia, J. Zhao, *Sens. Actuators B* **2010**, *146*, 98 – 102.
[238] Y. Xia, T. Fei, Y. He, R. Wang, F. Jiang, T. Zhang, *Mater. Lett.* **2012**, *66*, 19 – 21.
[239] P. Li, Y. Li, B. Ying, M. Yang, *Sens. Actuators B* **2009**, *141*, 390 – 395.
[240] M. Panapoy, W. Singsang, B. Ksapabutr, *Phys. Scr.* **2010**, *T139*, 014056.
[241] Z. Li, H. Zhang, W. Zheng, W. Wang, H. Huang, C. Wang, A. G. MacDiarmid, Y. Wei, *J. Am. Chem. Soc.* **2008**, *130*, 5036 – 5037.
[242] Q. Qi, T. Zhang, L. Wang, *Appl. Phys. Lett.* **2008**, *93*, 023105.
[243] H. Zhang, Z. Li, W. Wang, C. Wang, L. Liu, *J. Am. Ceram. Soc.* **2010**, *93*, 142 – 146.
[244] W. Wang, Z. Li, L. Liu, H. Zhang, W. Zheng, Y. Wang, H. Huang, Z. Wang, C. Wang, *Sens. Actuators B* **2009**, *141*, 404 – 409.
[245] Q. Qi, T. Zhang, S. Wang, X. Zheng, *Sens. Actuators B* **2009**, *137*, 649 – 655.
[246] Y.-F. Lin, J. Song, Y. Ding, S.-Y. Lu, Z. L. Wang, *Appl. Phys. Lett.* **2008**, *92*, 022105.
[247] M. Zhang, T. Gao, J. Wang, J. Liao, Y. Qiu, H. Xue, Z. Shi, Z. Xiong, L. Chen, *Nano Energy* **2015**, *11*, 510 – 517.
[248] X. Xiao, L. Yuan, J. Zhong, T. Ding, Y. Liu, Z. Cai, Y. Rong, H. Han, J. Zhou, Z. L. Wang, *Adv. Mater.* **2011**, *23*, 5440 – 5444.
[249] J. Fang, X. Wang, T. Lin, *J. Mater. Chem.* **2011**, *21*, 11088 – 11091.
[250] S. Choi, Z. Jiang, *Sens. Actuators A* **2006**, *128*, 317 – 326.
[251] L. T. Beringer, X. Xu, W. Shih, W.-H. Shih, R. Habas, C. L. Schauer, *Sens. Actuators A* **2015**, *222*, 293 – 300.
[252] L. Persano, C. Dagdeviren, Y. W. Su, Y. H. Zhang, S. Girardo, D. Pisignano, Y. G. Huang, J. A. Rogers, *Nat. Commun.* **2013**, *4*, 1633.
[253] J. W. Zhong, Y. Zhang, Q. Z. Zhong, Q. Y. Hu, B. Hu, Z. L. Wang, J. Zhou, *ACS Nano* **2014**, *8*, 6273 – 6280.
[254] J. Zhong, Q. Zhong, Q. Hu, N. Wu, W. Li, B. Wang, B. Hu, J. Zhou, *Adv. Funct. Mater.* **2015**, *25*, 1798 – 1803.
[255] Z. L. Wang, *Faraday Discuss.* **2014**, *176*, 447 – 458.
[256] M. Ha, J. Park, Y. Lee, H. Ko, *ACS Nano* **2015**, *9*, 3421 – 3427.
[257] V. Modafferi, G. Panzera, A. Donato, P. L. Antonucci, C. Cannilla, N. Donato, D. Spadaro, G. Neri, *Sens. Actuators B* **2012**, *163*, 61 – 68.
[258] T. Seesaard, P. Lorwongtragool, T. Kerdcharoen, *Sensors* **2015**, *15*, 1885 – 1902.

[259] N. L. Lala, V. Thavasi, S. Ramakrishna, *Sensors* **2009**, *9*, 86–101.
[260] A. Yang, X. Tao, R. Wang, S. Lee, C. Surya, *Appl. Phys. Lett.* **2007**, *91*, 133110.
[261] T. Kinkeldei, C. Zysset, N. Münzenrieder, G. Tröster, *Sens. Actuators B* **2012**, *174*, 81–86.
[262] K. M. Manesh, A. I. Gopalan, L. Kwang-Pill, P. Santhosh, S. Kap-Duk, L. Duk-Dong, *IEEE T. Nanotechnol.* **2007**, *6*, 513–517.
[263] Y. Gao, X. Li, J. Gong, B. Fan, Z. Su, L. Qu, *J. Phys. Chem. B* **2008**, *112*, 8215–8222.

Received: August 6, 2015
Published online: March 23, 2016

